

A DIAGRAMMATIC CATEGORY FOR GENERALIZED BOTT-SAMELSON BIMODULES AND A DIAGRAMMATIC CATEGORIFICATION OF INDUCED TRIVIAL MODULES FOR HECKE ALGEBRAS

OR: HOW I LEARNED TO STOP WORRYING AND CALCULATE SOME IDEMPOTENTS

BEN ELIAS

ABSTRACT. Let R be the polynomial ring of the reflection representation of $W = S_n$, and for any parabolic subgroup $W_J \subset W$ corresponding to a subset J of the Dynkin diagram, let R^J be the subring of polynomials invariant under W_J . When $J = \{i\}$ is a singleton, denote the ring R^i and the corresponding reflection s_i .

Previously in [3], the subcategory of R -bimodules generated monoidally by $R \otimes_{R^i} R$ for arbitrary i was given a diagrammatic presentation, so that morphisms may be viewed as labelled planar graphs. Here, a diagrammatic presentation is given for the subcategory generated by $R \otimes_{R^J} R$ for arbitrary J , extending the previous diagrammatics. In addition, a diagrammatic presentation is given for a certain subcategory of $R^J - R$ -bimodules which categorifies the representation of the Hecke algebra of W constructed by inducing the trivial representation of the Hecke algebra of W_J .

Whenever $x = s_{i_1} s_{i_2} \dots s_{i_d}$ is a reduced expression for the longest element of W_J , the R -bimodule $R \otimes_{R^J} R$ will be a direct summand of $M_x = R \otimes_{R^{i_1}} R \otimes_{R^{i_2}} R \otimes \dots \otimes_{R^{i_d}} R$. The key result is an explicit computation of the map $M_x \rightarrow M_y$, for two reduced expressions x, y of the longest element, given by projecting $M_x \rightarrow R \otimes_{R^J} R$ and including $R \otimes_{R^J} R \rightarrow M_y$. The construction of this map uses the higher Coxeter theory of Manin and Schechtman.

CONTENTS

1.	Introduction	2
2.	Background	6
3.	A Thicker Calculus	18
4.	Induced Trivial Representations	51
	References	55

1. INTRODUCTION

The Hecke algebra \mathcal{H} associated to a Dynkin diagram Γ is an algebra of fundamental importance. It (or its regular representation) can be viewed as the decategorification of the category \mathcal{P} of B -equivariant perverse sheaves on the flag variety, or as the decategorification of the associated category \mathcal{O} , and therefore the Hecke algebra encodes numerics associated to those categories. In the early 90s Soergel provided an additional categorification of the Hecke algebra, known as the category of Soergel Bimodules \mathcal{B} , which is far more accessible than the other two approaches, and can be effectively used to study them both. Soergel bimodules are bimodules over a polynomial ring, and as such, are attractively simple and explicit.

Let us restrict henceforth to finite type A Dynkin diagrams. Recently in [3], the author in conjunction with Mikhail Khovanov contributed to this explicitness by giving (in some sense) a diagrammatic presentation of \mathcal{B} . That is, every morphism in \mathcal{B} can be viewed as a linear combination of planar graphs with boundary (modulo graphical relations), and composition is given by stacking planar graphs on top of each other. For some basic introduction to planar diagrammatics for monoidal categories, we recommend chapter 4 of [8]. Planar graphs now provide a simple way to encode what are potentially very complicated maps of R -bimodules.

This paper continues the elaboration of categorified Hecke theory on several related fronts: by explicitly finding certain important idempotents in the category, by expanding the graphical calculus of [3] to a new class of objects, and by giving a diagrammatic presentation of a category which categorifies the induced trivial representations from sub-Dynkin diagrams.

Let R be the ring of polynomials on the Cartan subalgebra of the Dynkin diagram. It is a free polynomial ring with a number of generators equal to the number of vertices in Γ , graded so that linear polynomials have degree 2, and with a built-in action of the Weyl group W . To any subset of the Dynkin diagram J (which we call henceforth a *parabolic subset*) one may associate the parabolic subgroup $W_J \subset W$, and the ring of invariants $R^J \stackrel{\text{def}}{=} R^{W_J}$. When $J = \{i\}$ is a singleton, denote the invariant ring R^i . Let d_J be the length of the longest element w_J of W_J .

Soergel bimodules form a full subcategory of $R \otimes_{R^W} R\text{-mod}$, that is, the monoidal category of graded bimodules over R for which the right and left action of symmetric polynomials agree. Consider the bimodule $B_i \stackrel{\text{def}}{=} R \otimes_{R^i} R\{-1\}$, where $\{1\}$ denotes the grading shift. The category \mathcal{B}_{BS} of *Bott-Samelson bimodules* is the full subcategory generated by tensor products of B_i (and their grading shifts and direct sums). More generally, let $B_J \stackrel{\text{def}}{=} R \otimes_{R^J} R\{-d_J\}$. The category \mathcal{B}_{gBS} of *generalized Bott-Samelson bimodules* is the full subcategory generated by tensor products of B_J . It is known that B_J will occur as a summand of $B_{i_1} \otimes \dots \otimes B_{i_{d_J}}$ whenever $s_{i_1} \dots s_{i_{d_J}}$ is a reduced expression for w_J . The category \mathcal{B} of *Soergel bimodules* is the full subcategory generated by all summands of Bott-Samelson bimodules, or equivalently, all summands of generalized Bott-Samelson bimodules. The category \mathcal{B} has Grothendieck group isomorphic

to the Hecke algebra, where grading shift is sent to multiplication by v (viewing \mathcal{H} as a $\mathbb{Z}[v, v^{-1}]$ -algebra), and where $[B_i] = b_i$ the Kazhdan-Lusztig generators, and $[B_J] = b_J$ the Kazhdan-Lusztig basis elements corresponding to w_J . This is a result of Soergel, see [12, 13, 14].

In this paper we shall be interested in this process of adding direct summands, known as taking the *idempotent completion* or *Karoubi envelope*. Given an additive category one can identify “direct summands” by finding the idempotents which correspond to projections to those summands, and the Karoubi envelope is a way of formally adding these idempotents as new objects. Equivalently, one can view the category as an algebroid, and take the category of all projective right modules over that algebroid. For more background on the Karoubi envelope, see [1]. In order to speak reasonably about the Grothendieck group (or ring) of an additive (monoidal) category, we want it to be idempotent closed and have the Krull-Schmidt property. This will guarantee that isomorphism classes of indecomposable objects will form a basis for the Grothendieck group. Often, the easiest way to obtain such a category is to define a subcategory and then take the idempotent completion. This is the approach taken by Khovanov and Lauda in [5, 6] and Lauda in [8] where they give a diagrammatic category whose idempotent completion categorifies the quantum group. Similarly, in [3] a diagrammatic presentation is given for \mathcal{B}_{BS} , not for \mathcal{B} , and the latter is the idempotent completion of the former.

To pass from a diagrammatic presentation of a category to that of its idempotent completion is difficult. One must identify all the indecomposable idempotents, and pick out which idempotents give isomorphic summands. For the quantum group this is a tractable problem, for a couple reasons. One knows (thanks to [15] and the link with geometry) that the indecomposable objects descend to the canonical basis of the quantum group, which means that one needs only to find the idempotents corresponding to each basis element. These idempotents are typically easy to find: for instance, they are given explicitly for “divided powers” in [5]. Khovanov, Lauda, Mackaay, and Stošić [7] have presented the Karoubi envelope diagrammatically for $\text{sl}(2)$, which they refer to as the “thick calculus” because the new idempotents are represented by thick lines.

The same question is quite difficult for the Hecke algebra. It is currently unknown in general what basis of \mathcal{H} corresponds to the indecomposables in \mathcal{B} . The Soergel conjecture states that it is the *Kazhdan-Lusztig basis*, but this remains a conjecture in general. Even if we knew the truth of the Soergel conjecture, finding the idempotent in \mathcal{B}_{BS} corresponding to each element of the Kazhdan-Lusztig basis is non-trivial. What this paper does is provide partial results in this direction: we do know that the basis elements b_J lift to indecomposables B_J , and this paper identifies the idempotents which pick out B_J as a summand of $B_{i_1} \otimes \dots \otimes B_{i_{d_J}}$ for any reduced expression for w_J . This allows us to “thicken” our calculus somewhat, extending it to include all generalized Bott-Samelson bimodules as well. This calculus is still “incomplete” in some sense: it is a mathematically complete presentation for the category, but it is very likely that the calculus could be augmented further by more pictures and more relations so that

other properties of the category would become more intuitive. We have augmented it here as much as we currently know how.

To produce the idempotent corresponding to a parabolic subset J , we utilize Manin-Schechtman theory. Manin and Schechtman in [10] provide a beautiful and detailed study of a certain n -category associated with the symmetric group, which might be thought of as “higher Coxeter theory.” These results can be used to study the set of all reduced expressions for a particular element of the symmetric group, and give it the structure of a semi-oriented graph with a unique sink and a unique source up to equivalence. To an oriented path (or reverse-oriented path) in this graph we produce a map between Bott-Samelson bimodules, which does not depend on the oriented path chosen, only the beginning and end vertex. The map associated to a path which goes in oriented fashion from source to sink and then in reverse oriented fashion from sink to source will be the idempotent we seek, when we look at the graph for the longest element w_J . The connection between Manin-Schechtman theory and Soergel bimodules is potentially a can of very delicious worms. Nicolas Libedinsky independently studied a very similar question in [9], where he looks at morphisms induced by paths in the expression graph for an arbitrary element $w \in W$, but in the context not of the symmetric group but of *extra large* Coxeter groups ($m_{s,t} > 3$ for any indices s, t). For these Coxeter groups the expression graph is quite simple, and Manin-Schechtman theory does not apply. Libedinsky shows that the morphism corresponding to any path which hits every reduced expression is an idempotent, and that these idempotents pick out a single isomorphism class of direct summand.

The entire story of Soergel bimodules should be viewed in the larger context of singular Soergel bimodules, as introduced by Geordie Williamson in his thesis [16]. Singular Soergel bimodules form a 2-category: the objects are rings R^J for each parabolic subset $J \subset \Gamma$, and the Hom categories are some full subcategories of $R^J \otimes_{R^W} R^K\text{-mod}$. The 2-category of *generalized singular Bott-Samelson bimodules* is generated under tensor product by induction and restriction bimodules, for the inclusion $R^J \subset R^K$ of rings whenever $K \subset J$. Note that B_J can be viewed as the tensor product of an induction and a restriction, from $K = \emptyset$ to J and back to K . Taking the idempotent completion we obtain the 2-category of singular Soergel bimodules. This 2-category has Grothendieck category isomorphic to the *Hecke Algebroid*, an “idempotentized” version of the Hecke algebra. It has objects given by parabolic subsets J , and the Hom space from J to K is given by the intersection of the left ideal $\mathcal{H}b_K$ with the right ideal $b_J\mathcal{H}$. Multiplication is as in the Hecke algebra, except renormalized. This is proven and amply described in Williamson’s thesis. Soergel bimodules form the endomorphism category of the object $R = R^\emptyset$ inside the 2-category of singular Soergel bimodules.

The right (resp. left) trivial module of the Hecke algebra is a rank 1 $\mathbb{Z}[v, v^{-1}]$ -module where each b_i acts by multiplication by $[2] \stackrel{\text{def}}{=} (v + v^{-1})$. Because $b_i b_J = b_J b_i = [2] b_J$ whenever $i \in J$, one can show that the induced module to \mathcal{H} of the trivial module of the parabolic subalgebra \mathcal{H}_J is precisely the right (resp. left) ideal of \mathcal{H} generated by b_J . This, in turn, is exactly the Hom space from J to \emptyset (resp. from \emptyset to J) in the

Hecke algebroid. Therefore, this induced module already has a natural categorification, by the category $\text{Hom}(R^J, R)$ of singular Soergel bimodules. The right action of \mathcal{H} lifts to the right monoidal action of $\text{End}(R) = \mathcal{B}$ on $\text{Hom}(R^J, R)$ inside the 2-category. We note quickly that, since the composition is over \emptyset , there is no renormalization in the multiplication in the Hecke algebroid, so the reader may pretend for now that multiplication in the Hecke algebroid proceeds precisely as in the Hecke algebra. In order to categorify this induced trivial representation, it remains to find a diagrammatic description of $\text{Hom}(R^J, R)$.

This paper provides a diagrammatic presentation of $\text{Hom}_{\text{BS}}(R^J, R)$, the full subcategory of *J-singular Bott-Samelson bimodules*, which has $\text{Hom}(R^J, R)$ as its idempotent completion. A *J-singular Bott-Samelson bimodule* is just a usual Bott-Samelson R -bimodule with scalars restricted to R^J on one side. In order to motivate the presentation and prove that it works, we need some of the results stated earlier about the idempotent which picks out B_J . There is a (non-full) faithful functor from $\text{Hom}(R^J, R)$ to $\text{Hom}(R, R) = \mathcal{B}$ given by inducing on the left from R^J up to R . By inserting the idempotent appropriately, one gives a diagrammatic presentation of the image in \mathcal{B}_{BS} of $\text{Hom}_{\text{BS}}(R^J, R)$, and this allows us to prove everything we desire. However, the diagrammatic category for the induced trivial module is itself quite simple, and can be enjoyed in the absence of any knowledge of the idempotent or its properties.

Finding a diagrammatic presentation of the entire 2-category of generalized singular Bott-Samelson bimodules is a more difficult question, and is work in progress between the author and Williamson. The functor between the description given here of the small fragment $\text{Hom}_{\text{BS}}(R^J, R)$ and the description in progress of the full 2-category is actually rather simple and trivial, so we will not bother to explain it here, as it would require too much exposition of other work.

Having a categorification of induced trivial modules is a first step towards the categorification of Hecke representation theory in general. Much about the representation theory of the Hecke algebra can be understood using induced trivial and sign modules, and the Hom spaces between them. It is one of the author's goals to categorify this whole picture, although the work is still preliminary and it is too early to announce any results yet.

One should also point out that induced modules have been categorified before in much more generality, in the context of category \mathcal{O} , by Stroppel and Mazorchuk [11]. It is very likely that the category of this paper should be related to their categorification of the induced trivial module by applying Soergel's functor.

The structure of this paper is as follows. Chapter 2 contains the preliminary background material. The first two sections will state all the facts about the Hecke algebra (and algebroid) and the Soergel-Williamson categorification that we will need. The third section will be a lightning recollection of the diagrammatics for Soergel bimodules, and only introduces a little new notation at the end. The final section will be a discussion of what it means to add some direct summands to an additive category, and will outline the goal of the next chapter. Chapter 3 describes the idempotent in

question, and provides diagrammatics for the thicker calculus for \mathcal{B}_{gBS} . It begins with two sections on Manin-Schechtman theory, and continues with two sections of terrible computations, terminating in Theorems 3 and 4. We have done our best to make the computations readable, always doing things with examples and never in general form, but it may still be difficult to read through sections 3.3 and 3.4 without doing the computations oneself. Finally, section 3.5 provides diagrammatics for \mathcal{B}_{gBS} . After all this work, it is quite easy in Chapter 4 to provide diagrammatics for $\text{Hom}_{\text{BS}}(R^J, R)$.

Acknowledgments.

The author was supported by NSF grants DMS-524460 and DMS-524124, and would like to thank Mikhail Khovanov for his suggestions, and Geordie Williamson for many useful discussions.

2. BACKGROUND

We expect the reader to be familiar with [3] and will be extremely terse when recalling notation or definitions therefrom. It will be enough to have glanced through Chapters 2 and 3 of that paper; aside from that, we use only once the concept of one-color reduction, found in Chapter 4. Alternatively (perhaps preferably, thanks to the advent of color) one should read [2] chapters 2.1, 2.3 and 2.4. We change only the notation for the names of the categories, and change the variable t to v in order to be consistent with the papers of Soergel (wherein, for those who understand, $t = q^{\frac{1}{2}}$ and $v = q^{-\frac{1}{2}}$; in [3] we used t for $q^{-\frac{1}{2}}$ in some preliminary versions).

It may also be useful to the reader to be familiar with [16], at least the basic definitions and the statements of the main theorems. Perhaps the first three pages of the introduction will suffice. We will be terse in recalling this as well. We change notation in that we use the letter b to denote Kazhdan-Lusztig elements, instead of \underline{H} .

Let us fix some notation for the remainder of the paper.

Let $I = \{1, \dots, n\}$ index the vertices of the Dynkin diagram A_n ; elements of I will be called *indices* or *colors*. The terms *distant* and *adjacent* refer to the relative position of two indices in the Dynkin diagram, not in any word or picture. Let $W = S_{n+1}$ be the Coxeter group, with simple reflections s_i , $i \in I$, and let \mathcal{H} be the associated Hecke algebra over $\mathbb{Z}[v, v^{-1}]$. Let $R = \mathbb{k}[f_1, \dots, f_n]$ be the coordinate ring of the geometric representation, where f_i are the simple roots and \mathbb{k} is a field of characteristic $\neq 2$. The ring R is graded with $\deg(f_i) = 2$, and modules over R will be graded, even when we forget to say so. The grading shift will be denoted $\{1\}$.

To a *parabolic subset* $J \subset I$ we let W_J, \mathcal{H}_J, R_J denote the corresponding objects. We let w_J be the longest element of W_J , and d_J its length. We say that an index i is *distant* from a parabolic subset J if it is distant from all the indices in J , and we say two parabolic subsets are *distant* if all the indices in one are distant from the indices in the other. We let $[J]$ denote the Hilbert polynomial of W_J , defined by $v^{-d_J} \sum_{w \in W_J} v^{2l(w)}$. It is denoted $\pi(J)$ in [16]. For instance, the Hilbert polynomial of S_n is $[n]!$, quantum n factorial.

When we write $\mathrm{HOM}(X, Y)$ for X, Y two objects in a graded category, we refer to the graded vector space which is $\oplus_{n \in \mathbb{Z}} \mathrm{Hom}(X, Y\{n\})$. Note that when X, Y are graded $S - T$ -bimodules for two commutative rings S, T , the graded vector space $\mathrm{HOM}(X, Y)$ is also a graded $S - T$ -bimodule.

All the results below which are attributed to Soergel may be found in [14]. Many of Soergel's other papers (see [12, 13]) are relevant and may have proven the same result first, but this paper has the advantage of being purely algebraic. All the results below which are attributed to Williamson may be found in [16]. More information on any of the topics in the first two sections can be found in those papers.

2.1. The Hecke algebra and algebroid. The Hecke algebra \mathcal{H} has a presentation as an algebra over $\mathbb{Z}[v, v^{-1}]$ with generators b_i , $i \in I$ and the *Hecke relations*

$$(2.1) \quad b_i^2 = (v + v^{-1})b_i$$

$$(2.2) \quad b_i b_j = b_j b_i \text{ for distant } i, j$$

$$(2.3) \quad b_i b_j b_i + b_j = b_j b_i b_j + b_i \text{ for adjacent } i, j.$$

There is a basis for \mathcal{H} known as the *Kazhdan-Lusztig basis*, with one element b_w for each $w \in W$. We will not write them down explicitly in terms of the generators, nor is it easy to do so. However, we note that when $w = w_J$ is the longest element of a parabolic subgroup, the corresponding basis element $b_J \stackrel{\mathrm{def}}{=} b_{w_J}$ does have a simple presentation in another basis known as the *standard basis*. See [16] for more details. We also note that b_J is contained inside the subalgebra \mathcal{H}_J , i.e. it is generated by b_i for $i \in J$. When $J = \{i\}$ is a singleton, $b_J = b_i$; when J is empty, $b_\emptyset = 1$. The key properties satisfied by b_J are the following generalizations of (2.1) and (2.2):

$$(2.4) \quad b_i b_J = b_J b_i = (v + v^{-1})b_J \text{ for any } i \in J$$

$$(2.5) \quad b_J b_K = b_K b_J = [J] b_K \text{ whenever } J \subset K$$

$$(2.6) \quad b_i b_J = b_J b_i \text{ for any } i \text{ distant from } J.$$

$$(2.7) \quad b_J b_K = b_K b_J = b_{J \amalg K} \text{ for distant } J, K.$$

Several points deserve emphasis. Equation 2.4 implies that the left or right ideal of b_J inside \mathcal{H}_J is rank 1 as a $\mathbb{Z}[v, v^{-1}]$ -module, spanned by b_J . In addition, if x is any element in a \mathcal{H} -module for which $b_i x = (v + v^{-1})x$ for any $i \in J$, it must be the case that $b_J x = [J]x$ (this is more obvious in the standard basis; see [16], Lemma 2.2.3). Thus equation (2.4) implies (2.5). In particular, if $x \in \mathcal{H}$ is such an element then it must be in the right ideal of b_J (after inverting $[J]$ in $\mathbb{Z}[v, v^{-1}]$). Putting these observations together, one may identify b_J as the unique element x (up to scalar) which is contained in \mathcal{H}_J and for which $b_i x = [2]x$ for any $i \in J$.

The Hecke algebroid \mathfrak{H} is a $\mathbb{Z}[v, v^{-1}]$ -linear category with objects labelled by parabolic subsets. Henceforth, whenever we write $\mathrm{Hom}(J, K)$ for two parabolic subsets, we always

refer to the Hom space in \mathfrak{H} . The $\mathbb{Z}[v, v^{-1}]$ -module $\text{Hom}(J, K)$ is the intersection in \mathcal{H} of the left ideal $\mathcal{H}b_J$ with the right ideal $b_K\mathcal{H}$. Composition from $\text{Hom}(J, K) \times \text{Hom}(L, J) \rightarrow \text{Hom}(L, K)$ is given by renormalized multiplication in the Hecke algebra, i.e. $x \circ y = \frac{xy}{[J]}$. From this, it is clear that b_J is the identity element of $\text{End}(J)$. It is also clear that $\text{End}(\emptyset) = \mathcal{H}$ as an algebra. Whenever $J \subset K$, b_K is in both the right and left ideal of b_J , and therefore there is an inclusion of ideals $\text{Hom}(K, L) \subset \text{Hom}(J, L)$. This inclusion is realized by precomposition with $b_K \in \text{Hom}(J, K)$. A similar statement can be made about $\text{Hom}(L, K) \subset \text{Hom}(L, J)$ and postcomposition with $b_K \in \text{Hom}(K, J)$.

We will care in this paper primarily about the case of $\text{Hom}(J, \emptyset)$ (resp. $\text{Hom}(\emptyset, J)$) for some J . This is none other than the left (resp. right) ideal generated by b_J inside \mathcal{H} , and the left (resp. right) action of $\text{End}(\emptyset)$ on this space by composition is precisely the action of \mathcal{H} on the ideal. Henceforth, every result stated for the left, or for $\text{Hom}(J, \emptyset)$ etcetera, has an obvious analog on the right, which we leave to the reader.

The Hecke algebra has a *trivial representation* T , a left \mathcal{H} -module. It is free of rank 1 as a $\mathbb{Z}[v, v^{-1}]$ -module, and b_i acts by multiplication by $(v + v^{-1})$. As is clear by (2.4), the trivial representation can be embedded inside the regular representation of \mathcal{H} by looking at the left ideal of b_I . For a parabolic subset $J \subset I$, we may induce the trivial representation of \mathcal{H}_J up to \mathcal{H} to get a representation T_J , and this can also (less obviously) be embedded inside the regular representation of \mathcal{H} by looking at the left ideal of b_J . Therefore, this induced trivial module is none other than $\text{Hom}(J, \emptyset)$.

2.2. The Soergel-Williamson categorification. In order to categorify the Hecke algebra within the category of R -bimodules, we may wish to find R -bimodules B_i , $i \in I$, which satisfy

$$(2.8) \quad B_i \otimes B_i \cong B_i\{1\} \oplus B_i\{-1\}$$

$$(2.9) \quad B_i \otimes B_j \cong B_j \otimes B_i \text{ for distant } i, j$$

$$(2.10) \quad B_i \otimes B_j \otimes B_i \oplus B_j \cong B_j \otimes B_i \otimes B_j \oplus B_i \text{ for adjacent } i, j.$$

One could then define a map from \mathcal{H} to the split Grothendieck ring of R -bimodules by sending b_i to $[B_i]$. In order to categorify various aspects of the Hecke algebroid, one may also seek R -bimodules B_J for each parabolic set J , which satisfy

$$(2.11) \quad B_J \otimes B_i \cong B_i \otimes B_J \cong B_J\{1\} \oplus B_J\{-1\} \text{ whenever } i \in J.$$

$$(2.12) \quad B_J \otimes B_K \cong B_K \otimes B_J \cong [J] B_K \text{ whenever } J \subset K$$

$$(2.13) \quad B_J \otimes B_K \cong B_K \otimes B_J \cong B_{J \amalg K} \text{ for distant } J, K.$$

Here, we use the shorthand that $[J] B_K$ indicates a direct sum of many copies of B_K with the appropriate degree shifts. The isomorphism (2.11) could be rewritten $B_J \otimes B_i \cong [2] B_J$, for instance.

Potentially, these B_J could be the image of b_J under the map above. In fact, these modules exist, and we shall describe them explicitly in a larger context. For a more thorough study of this material, see Williamson's thesis [16] where this was first fully described.

Everything lives within the 2-category **Bim**, where the objects are rings, and the morphism category between two rings $\text{Hom}(R, S)$ is the category of $S - R$ -bimodules. Composition of 1-morphisms is given by the tensor product of bimodules. As usual, all rings and bimodules are graded but we don't bother to mention it. We will describe several 2-subcategories of **Bim**.

The ring R has a natural action of W , and so for each parabolic subset J we have a subring $R^J \stackrel{\text{def}}{=} R^{W_J}$ of invariants. When $J = \{i\}$ is a single element subset, we abbreviate the invariant ring as R^i . Whenever $J \subset K$ we have $R^K \subset R^J$, and therefore R^J can be viewed as an R^K module on either the right or the left. Viewing R^J as an $R^K - R^J$ -bimodule or vice versa, tensoring with it will correspond to either induction or restriction, between R^K -modules and R^J -modules.

Consider the full (additive graded) 2-subcategory $\mathfrak{B}_{\text{temp}}$ of **Bim** whose objects are the various R^J for each parabolic J , and whose 1-morphisms are generated by induction and restriction bimodules. That is, to an arbitrary sequence of parabolic subsets $J_1 \subset K_1 \supset J_2 \subset K_2 \supset \dots \subset K_d \supset J_{d+1}$ we may associate the $R^{J_1} - R^{J_{d+1}}$ -bimodule $R^{J_1} \otimes_{R^{K_1}} R^{J_2} \otimes_{R^{K_2}} \dots \otimes_{R^{K_d}} R^{J_{d+1}}$. We call such a bimodule (for lack of a better name) a *generalized (singular) Bott-Samelson bimodule*; these generate $\mathfrak{B}_{\text{temp}}$. The idempotent completion of $\mathfrak{B}_{\text{temp}}$ will be called the 2-category of *(singular) Soergel Bimodules* and denoted \mathfrak{B} . That is, in $\text{Hom}_{\mathfrak{B}}(R^J, R^K)$ we include all bimodules of the above form, as well as direct summands thereof. Let us write henceforth $\text{Hom}(R^J, R^K)$ for the Hom category in \mathfrak{B} , and $\text{Hom}_{\text{temp}}(R^J, R^K)$ for the Hom category in $\mathfrak{B}_{\text{temp}}$. The category $\text{Hom}(R^\emptyset, R^\emptyset)$, a full subcategory of R -bimodules, will be denoted \mathcal{B} and called the category of *Soergel bimodules*. We will add the word singular when necessary to indicate that bimodules need not necessarily be over R , but can be over invariant subrings.

We can define several full (additive graded monoidal) subcategories of \mathcal{B} . Firstly we have $\mathcal{B}_{\text{temp}} = \text{Hom}_{\text{temp}}(R^\emptyset, R^\emptyset)$, which is generated by those modules associated to sequences as above where $J_1 = \emptyset = J_{d+1}$. We will not care for this category in this paper. We also have the subcategory of \mathcal{B} generated by those sequences where each $J_m = \emptyset$; we call this \mathcal{B}_{BS} , the category of *generalized Bott-Samelson bimodules*. This subcategory is generated monoidally by bimodules $B_J \stackrel{\text{def}}{=} R \otimes_{R^J} R\{-d_J\}$ for each J . For a sequence $\underline{j} = J_1 J_2 \dots J_d$ of parabolic subsets, we denote by $B_{\underline{j}}$ the bimodule $B_{J_1} \otimes B_{J_2} \dots \otimes B_{J_d} = R \otimes_{R^{J_1}} R \otimes_{R^{J_2}} \dots \otimes_{R^{J_d}} R\{-\sum d_{J_m}\}$. Finally, we may consider the subcategory \mathcal{B}_{BS} generated by those sequences where each $J_m = \emptyset$ and each K_m is a singleton. These are generated by $B_i \stackrel{\text{def}}{=} B_{\{i\}} = R \otimes_{R^i} R\{-1\}$, and are called *Bott-Samelson bimodules*. These correspond to sequences $\underline{i} = i_1 i_2 \dots i_d$ of indices, and are the "original" Bott-Samelson bimodules after whom all the generalizations are named.

Notation 2.1. Unless stated otherwise, \underline{i} will be a sequence of indices, not of general parabolic subsets. We let $b_{\underline{i}}$ be the corresponding product of the generators b_i in \mathcal{H} , and $s_{\underline{i}}$ be the corresponding product of s_i in W . We write $d(\underline{i})$ for the length of the sequence.

It is fairly clear that the objects B_i , or more generally B_J , are all themselves indecomposable as R -bimodules. The category $\mathcal{B}_{\text{temp}}$ is complicated, but \mathcal{B}_{BS} is much simpler, and it contains sufficient information, as shown by the following result of Soergel.

Claim 2.2. *Every Soergel bimodule is a summand of a Bott-Samelson bimodule.*

Since Soergel bimodules form an idempotent-closed subcategory of a bimodule category, it has the Krull-Schmidt property and its (additive) Grothendieck group will be generated freely by indecomposables. Note that none of the categories mentioned are abelian, and we are always taking the additive or split Grothendieck group.

It is not hard to see that the bimodules B_i and B_J satisfy the desired properties above, and we can even be explicit. The isomorphism (2.8) can be deduced from the fact that, as an R^i -bimodule, $R \cong R^i \oplus R^i\{2\}$. This isomorphism is given explicitly using the Demazure operator $\partial_i: R \rightarrow R^i$, where $\partial_i(P) = \frac{P - s_i(P)}{f_i}$. This operator is R^i -linear, has degree -2, and sends $f_i \mapsto 2$ and $R^i \subset R$ to zero. The two projection operators from R to R^i are $P \mapsto \partial_i(P)$ and $P \mapsto \partial_i(Pf_i)$, of degrees -2 and 0 respectively; the inclusion operators are $Q \mapsto \frac{1}{2}f_iQ$ and $Q \mapsto \frac{1}{2}Q$, of degrees +2 and 0 respectively. We invite the reader to figure out the projections and inclusions for (2.8), or to look them up in [3]. The Demazure operator also provides an easy way to define the projection and inclusion operators for the splitting in (2.11).

To construct the isomorphism of (2.13), namely $R \otimes_{R^J} R \otimes_{R^K} R\{-d_J - d_K\} = B_J \otimes B_K \cong B_{J \sqcup K} = R \otimes_{R^{J \sqcup K}} R\{-d_J - d_K\}$ when J, K are distant, we note that any polynomial in R can be decomposed into polynomials symmetric in either W_J or W_K , so that the left side is spanned by elements $f \otimes 1 \otimes g$ for $f, g \in R$. The isomorphism sends $f \otimes 1 \otimes g \mapsto f \otimes g$.

The following theorems and results are due to Soergel and Williamson.

Theorem 1. (See [14] Proposition 5.7 or [16] Theorem 4.1.5) *The Grothendieck ring of \mathcal{B} is isomorphic to \mathcal{H} , where the isomorphism is defined by sending b_i to $[B_i]$ and v to $[R\{1\}]$. Under this isomorphism, b_J is sent to $[B_J]$.*

The isomorphism between \mathcal{H} and the Grothendieck ring of \mathcal{B} lifts to an isomorphism between \mathfrak{H} and the Grothendieck category of \mathfrak{B} . In this isomorphism, $R^J \in \text{Hom}(R^J, R^K)$ for $J \subset K$ has class equal to $b_K \in \text{Hom}(J, K)$. Said another way, induction categorifies the inclusion of ideals in \mathcal{H} , i.e. the functor $R^J \otimes_{R^K} (\cdot)$ categorifies $\text{Hom}(L, K) \hookrightarrow \text{Hom}(L, J)$. This functor is faithful, though not full; however, if X, Y are two $R^K - R^L$ -bimodules in $\text{Hom}(R^L, R^K)$ then $R^J \otimes_{R^K} \text{HOM}(X, Y) \cong \text{HOM}(R^J \otimes_{R^K} X, R^J \otimes_{R^K} Y)$. Similarly, restriction categorifies multiplication by $v^{d_K - d_J} b_K$, as a map into the ideal of b_K (NB: there is a “degree shift” built into restriction, unlike induction).

Claim 2.3. *Any singular Soergel bimodule in $\text{Hom}(R^J, R^K)$ is free as a left R^J -module and as a right R^K -module.*

Proof. This can be easily deduced from the same fact for the induction and restriction bimodules. \square

The Hecke algebra is equipped with a canonical $\mathbb{Z}[v, v^{-1}]$ -linear *trace* map $\varepsilon: \mathcal{H} \rightarrow \mathbb{Z}[v, v^{-1}]$, which picks out the coefficient of 1 in the standard basis of \mathcal{H} . It satisfies $\varepsilon(b_{\underline{i}}) = v^{d(\underline{i})}$ when \underline{i} has no repeated indices, and $\varepsilon(b_J) = v^{d_J}$ where d_J is the length of W_J . The Hecke algebra also has an antilinear antiinvolution ω , satisfying $\omega(v^a b_{\underline{i}}) = v^{-a} b_{\omega(\underline{i})}$ where $\omega(\underline{i})$ is the sequence run in reverse. Together, these induce a pairing on \mathcal{H} via $(x, y) = \varepsilon(y\omega(x))$.

Proposition 2.4. (See [14] Theorem 5.15 or [16] Theorem 5.2.2) *This canonical pairing is induced by the categorification \mathcal{B} , in that the graded rank of $\mathrm{HOM}_{\mathcal{B}}(X, Y)$ as a free left (or right) R -module is precisely $([X], [Y])$. Similarly, there is a formula for the graded ranks between two objects in $\mathrm{Hom}(R^J, R^K)$, as right R^J -modules or left R^K -modules.*

It is known that the indecomposables of \mathcal{B} are in bijection with W , and that they form a basis of \mathcal{H} . It is not known what the indecomposables actually are, or what basis of \mathcal{H} they descend to! One might hope that one obtains the Kazhdan-Lusztig basis, but this is a difficult question, known as the Soergel conjecture (see [14]). It is known from Soergel's work that the indecomposable corresponding to w is a direct summand of $B_{\underline{i}}$ whenever $s_{\underline{i}}$ is a reduced expression for w . However, finding the idempotent in $\mathrm{End}(B_{\underline{i}})$ corresponding to that indecomposable is difficult. This difficulty prevents one from coming up with diagrammatics for all of \mathcal{B} ; the diagrammatics in [3] are for the simpler category $\mathcal{B}_{\mathrm{BS}}$. There are other indecomposables one can identify, but the easiest ones to pick out are the B_J for various J . Most of the work in this paper will be devoted to finding the idempotent for B_J , which will allow us to produce diagrammatics for $\mathcal{B}_{\mathrm{BS}}$.

Putting together the previous theorems, we can state the following useful lemma, which tells us when an idempotent in $\mathrm{End}(B_{\underline{i}})$ will pick out B_J .

Lemma 2.5. *Let X be a summand of $B_{\underline{i}}$ for some sequence \underline{i} using only indices in J . Suppose that X satisfies $X \otimes B_i \cong X\{1\} \oplus X\{-1\}$ for all $i \in J$. Then the class of X in \mathcal{H} is a scalar multiple of b_J , and this scalar is the graded rank of the free R -module $\mathrm{HOM}(R, X)$, divided by v^{d_J} .*

Proof. Whatever $[X]$ is, it is contained in \mathcal{H}_J and satisfies $[X]b_i = (v + v^{-1})[X]$, so it satisfies the two criteria mentioned in Section 2.1 for being a scalar multiple of b_J . Since $\mathrm{HOM}(R, X)$ has graded rank $\varepsilon([X])$ and $\varepsilon(b_J) = v^{d_J}$, we can determine the scalar from this graded rank by dividing by v^{d_J} . \square

There is one more category to describe. The statement that $\mathrm{Hom}(R, R) = \mathcal{B}$ boils down to the claim that all direct summands of various inductions and restrictions to arbitrary parabolic subsets are in fact direct summands of bimodules $B_{\underline{i}}$, inductions and restrictions to singletons. This allows us to study the simpler category $\mathcal{B}_{\mathrm{BS}}$, which is the category drawn diagrammatically in [3]. We want a simpler category for $\mathrm{Hom}(R^J, R)$ as well, since this will categorify the left \mathcal{H} -module T_J . Let us define the full subcategory of $R^J - R$ -bimodules given by objects $\mathrm{Res} B_{\underline{i}}$, where this R -bimodule is restricted to

become an R^J -module on the left, as $\text{Hom}_{\text{BS}}(R^J, R)$ the category of J -singular Bott-Samelson bimodules.

Claim 2.6. *The idempotent completion of $\text{Hom}_{\text{BS}}(R^J, R)$ is $\text{Hom}(R^J, R)$.*

Proof. Using the classification theorem of indecomposables in \mathfrak{B} (see [16] Theorem 5.4.2) we know there is one indecomposable for each coset of W_J in W . Let $s_{\underline{i}}$ be a reduced expression for the minimal element w of that coset, and consider the restriction of $B_{\underline{i}}$. Using the support filtration (see [16]), it is clear that this module has the indecomposable corresponding to that coset appearing as a summand with multiplicity 1. (Thanks to Williamson for this proof.) \square

We will provide diagrammatics for the category $\text{Hom}_{\text{BS}}(R^J, R)$ in Chapter 4.

2.3. Soergel diagrammatics. In [3], the author and M. Khovanov give a diagrammatic presentation of \mathcal{B}_{BS} by generators and relations. Technically, the presentation is for a slightly different category: the (non-additive non-graded) monoidal category generated by B_i in the category of (non-graded) R -bimodules. In other words, instead of allowing grading shifts of $B_{\underline{i}}$ but restricting to degree 0 homogeneous maps, we don't allow grading shifts but allow all maps, making Hom spaces into a graded vector space. We also do not allow direct sums of various objects $B_{\underline{i}}$. One can recover the category \mathcal{B}_{BS} by taking the additive grading closure, which is a completely trivial procedure. There is no need to repeatedly belabor this point, so we will abuse notation and speak of such a thing as a diagrammatic presentation for \mathcal{B}_{BS} .

What follows is a brief summary of sections 2.3 and 2.4 of [2]. If this is the reader's first encounter with Soergel diagrammatics, we recommend reading those sections instead, as a better introduction. We will assume that many of the ideas found there are known to the reader, including biadjointness, dot forcing rules, idempotent decompositions, and one-color reductions. One can also see [3] for a less pretty version, but a version where the equivalence between these pictures and R -bimodules is explicitly defined.

An object in the diagrammatic version of \mathcal{B}_{BS} is given by a sequence of indices \underline{i} , which is visualized as d points on the real line \mathbb{R} , labelled or "colored" by the indices in order from left to right. These objects are also called $B_{\underline{i}}$. Morphisms from \underline{i} to \underline{j} are planar graphs in $\mathbb{R} \times [0, 1]$, with each edge colored by an index, with bottom boundary \underline{i} and top boundary \underline{j} , constructed out of univalent vertices (degree +1), trivalent vertices joining 3 edges of the same color (degree -1), 4-valent vertices joining edges of alternating distant colors (degree 0), and 6-valent vertices joining edges of alternating adjacent colors (degree 0).

We will occasionally use a shorthand to represent double dots. We identify a double dot colored i with the polynomial $f_i \in R$, and to a linear combination of disjoint unions of double dots in the same region of a graph, we associate the appropriate linear combination of products of f_i . For any polynomial $f \in R$, a square box with a polynomial f in a region will represent the corresponding linear combination of graphs

with double dots. We have an bimodule action of R on morphisms by placing boxes (i.e. double dots) in the leftmost or rightmost regions of a graph.

For instance,  $=$ $\boxed{f_i^2 f_j}$.

In the following relations, blue representing a generic index.

$$(2.14) \quad \begin{array}{c} \diagup \\ \diagdown \end{array} = \begin{array}{c} \diagdown \\ \diagup \end{array}$$

$$(2.15) \quad \begin{array}{c} \diagup \\ \diagdown \end{array} \bullet = | = \begin{array}{c} \bullet \\ \diagdown \end{array}$$

$$(2.16) \quad \bigcirc = 0$$

$$(2.17) \quad \begin{array}{c} \bullet \\ | \end{array} + \begin{array}{c} | \\ \bullet \end{array} = 2 \begin{array}{c} \bullet \\ | \end{array}$$

We have the following implication of (2.17):

$$(2.18) \quad || = \frac{1}{2} \left(\begin{array}{c} \bullet \\ \diagup \end{array} + \begin{array}{c} \diagdown \\ \bullet \end{array} \right).$$

In the following relations, the two colors are distant.

$$(2.19) \quad \text{crossing of blue and green lines} = ||$$

$$(2.20) \quad \text{blue line with green dot} = \text{green line with blue dot}$$

$$(2.21) \quad \text{blue Y-junction with green line} = \text{green Y-junction with blue line}$$

$$(2.22) \quad \begin{array}{c} \bullet \\ | \end{array} = \begin{array}{c} | \\ \bullet \end{array}$$

In this relation, two colors are adjacent, and both distant to the third color.

$$(2.23) \quad \text{triple crossing of blue, green, and red lines} = \text{triple crossing of blue, green, and red lines}$$

In this relation, all three colors are mutually distant.

$$(2.24) \quad \begin{array}{c} \text{green} \\ \diagup \diagdown \\ \text{blue} \end{array} = \begin{array}{c} \text{blue} \\ \diagup \diagdown \\ \text{green} \end{array}$$

Remark 2.7. Relations (2.19) thru (2.24) indicate that any part of the graph colored i and any part of the graph colored j “do not interact” for i and j distant. That is, one may visualize sliding the j -colored part past the i -colored part, and it will not change the morphism. We call this the *distant sliding property*.

In the following relations, the two colors are adjacent.

$$(2.25) \quad \begin{array}{c} \text{blue} \\ \diagup \diagdown \\ \text{red} \end{array} = \begin{array}{c} \text{red} \\ \diagup \diagdown \\ \text{blue} \end{array} + \begin{array}{c} \text{red} \\ \diagup \diagdown \\ \text{red} \end{array}$$

$$(2.26) \quad \begin{array}{c} \text{blue} \\ \diagup \diagdown \\ \text{blue} \end{array} = \begin{array}{c} \text{red} \\ \diagup \diagdown \\ \text{red} \end{array} - \begin{array}{c} \text{blue} \\ \diagup \diagdown \\ \text{blue} \end{array}$$

$$(2.27) \quad \begin{array}{c} \text{blue} \\ \diagup \diagdown \\ \text{red} \end{array} = \begin{array}{c} \text{red} \\ \diagup \diagdown \\ \text{blue} \end{array}$$

$$(2.28) \quad \begin{array}{c} \text{red} \\ \diagup \diagdown \\ \text{red} \end{array} - \begin{array}{c} \text{blue} \\ \diagup \diagdown \\ \text{blue} \end{array} = \begin{array}{c} \text{blue} \\ \diagup \diagdown \\ \text{blue} \end{array} - \begin{array}{c} \text{red} \\ \diagup \diagdown \\ \text{red} \end{array}$$

We have the following implication of the above:

$$(2.29) \quad \begin{array}{c} \text{blue} \\ \diagup \diagdown \\ \text{red} \end{array} = \begin{array}{c} \text{red} \\ \diagup \diagdown \\ \text{blue} \end{array}$$

In this final relation, the colors have the same adjacency as $\{1, 2, 3\}$.

$$(2.30) \quad \begin{array}{c} \text{blue} \\ \diagup \diagdown \\ \text{red} \end{array} = \begin{array}{c} \text{red} \\ \diagup \diagdown \\ \text{blue} \end{array}$$

There is a functor from this diagrammatically defined category to the category of R -bimodules, whereby a diagram unambiguously represents a specific bimodule map. The functor preserves the left and right R action on morphisms.

Theorem 2 (Main Theorem of [3]). *There is an equivalence of categories between this diagrammatic category and \mathcal{B}_{BS} , the category of Bott-Samelson bimodules.*

You can start paying attention again NOW.

The only facts about the functor to bimodules just mentioned that need to be recalled are in this paragraph. Let $1 \otimes 1 \otimes \dots \otimes 1 \in B_i$ be called a *1-tensor*. Then the 6-valent vertex and the 4-valent vertex both send 1-tensors to 1-tensors. So does the dot, positioned so that it represents a map from $B_i \rightarrow R$, and the trivalent vertex, positioned so that it represents a map from $B_i \rightarrow B_i \otimes B_i$. When the trivalent vertex is positioned so that it represents a map from $B_i \otimes B_i \rightarrow B_i$, the corresponding map of bimodules will simply apply the Demazure operator ∂_i to the middle term in $R \otimes_{R^i} R \otimes_{R^i} R$. Finally, the 6-valent vertex is a projector, as described below.

The relation (2.26) expresses the first direct sum decomposition below, while flipping the colors yields the second. Here, blue is i , red is $i+1$, and $J = \{i, i+1\}$.

$$(2.31) \quad B_i \otimes B_{i+1} \otimes B_i = B_J \oplus B_i$$

$$(2.32) \quad B_{i+1} \otimes B_i \otimes B_{i+1} = B_J \oplus B_{i+1}.$$

That is, the identity $\text{id}_{i(i+1)i}$ is decomposed into orthogonal idempotents. The first idempotent, which we call a *doubled 6-valent vertex*, is the projection from $B_i \otimes B_{i+1} \otimes B_i$ to its summand B_J . The 6-valent vertex itself is the projection from $B_i \otimes B_{i+1} \otimes B_i$ to B_J and then the inclusion into $B_{i+1} \otimes B_i \otimes B_{i+1}$.

We call the following map, which is the projection from $B_i \otimes B_{i+1} \otimes B_i$ to the “wrong” summand, by the name *aborted 6-valent vertex*.



Because projections to different summands are orthogonal, we have the following key equation, a simple consequence of (2.25), (2.14) and (2.16):

$$(2.33) \quad \text{Diagram of a 6-valent vertex with a blue line entering from the top, a red line entering from the bottom, and a blue line exiting from the bottom} = 0$$

We consistently use the following conventions for the rest of the paper. We use the colors blue, red, green, purple, and black to represent the indices 1, 2, 3, 4, 5 respectively.



When we have fixed a parabolic subset $J \subset I$ and wish to express an arbitrary index $i \in J$, we use either the color teal or brown.



2.4. Thickening. Our goal in this paper will be to provide diagrammatic presentations of both \mathcal{B}_{gBS} and $\text{Hom}_{\text{BS}}(R^J, R)$. The former will provide more intuition into Soergel bimodules in general; the latter will be a diagrammatic categorification of the induced trivial module T_J . The diagrammatic presentation of the latter is a fairly easy thing in its own right, but to really grok it, it will be better to understand \mathcal{B}_{gBS} first.

The goal of the ultimate paper would be to provide a diagrammatic presentation of \mathcal{B} . Passing from a diagrammatic presentation of a category to a presentation of its idempotent completion is no simple matter. One must classify all idempotents, and understand which idempotents are indecomposable and which isomorphic. For \mathcal{B}_{BS} , an understanding of all idempotents is still out of reach. However, if one does understand some idempotents, one can add them to the category to get a partial idempotent completion. In this section we will discuss a number of obvious facts about partial idempotent completions, presenting them in detail.

Definition 2.8. Let \mathcal{C} be a full subcategory of an ambient module category. By assuming this, we guarantee that the idempotent completion is fairly nice (Krull-Schmidt); in particular, it is also embedded in the same ambient category. If \mathcal{S} is a set of objects in the idempotent completion of \mathcal{C} , we let $\mathcal{C}(\mathcal{S})$ be the full subcategory of the ambient module category whose objects are those of \mathcal{C} as well as \mathcal{S} . We call this a *partial idempotent completion* or a *thickening* of \mathcal{C} . When \mathcal{S} consists of a single object M , we denote the thickening by $\mathcal{C}(M)$.

Let us assume that we have a description of all morphisms in \mathcal{C} , by generators and relations, and that M is a module in the idempotent completion. We may pick out M by using a particular idempotent φ_X inside some object $X \in \mathcal{C}$ of which M is a summand.

Claim 2.9. *To obtain a presentation of $\mathcal{C}(M)$ by generators and relations, we may take as generators the generators of \mathcal{C} along with two new maps $p_X: X \rightarrow M$ and $i_X: M \rightarrow X$, and as relations the relations of \mathcal{C} along with $i_X p_X = \varphi_X$ and $p_X i_X = \mathbb{1}_M$.*

Proof. This is a tautological fact about idempotent completions, which we spell out this once. By definition, $\text{Hom}_{\mathcal{C}(M)}(M, Y) = \text{Hom}_{\mathcal{C}}(X, Y)\varphi_X$, that is, those morphisms $X \rightarrow Y$ which are unchanged under precomposition by φ_X . The map i_X corresponds to $\varphi_X \in \text{End}(X)$ itself, and in the thickening, all maps from $M \rightarrow Y$ will clearly be compositions of i_X with some map $X \rightarrow Y$. Similar dual statements may be made about p_X and maps to M . Therefore i_X, p_X are the only new generators required. Any relations among maps factoring through M arise from relations for maps factoring through X (by definition of morphisms in $\mathcal{C}(M)$) and these can all be deduced using the relations stated above. \square

While this is sufficient to describe $\mathcal{C}(M)$, the result is not necessarily an intuitive description. The object M may have a variety of interesting maps to various objects in \mathcal{C} , whose properties could be deduced solely from the properties of φ_X , but which are not obvious *a priori*. For instance, it is not even obvious which other objects Y might have M as a summand.

One thing we can do is augment our presentation (or diagrammatics) by adding new symbols for certain maps which can be constructed out of maps in \mathcal{C} and the new maps p_X, i_X . That is, we add a new generator paired with a new relation which defines the new generator in terms of the existent morphisms. We can then deduce some relations which hold among these new symbols, by checking them in $\mathcal{C}(M)$. In doing so, one need not worry about the eternal questions one faces when given a presentation: do we have enough relations? Do we have too many? We already have a presentation, and we are merely adding new symbols and relations as a more intuitive shorthand.

One useful such augmentation will be to produce inclusions and projections for other objects Y of which M is a direct summand, using only the maps i_X, p_X and maps in \mathcal{C} .

Claim 2.10. *Given a summand M of X defined by idempotent φ_X , M will also be a summand of Y if and only if there exist maps $\varphi_{X,Y}: X \rightarrow Y$ and $\varphi_{Y,X}: Y \rightarrow X$ such that $\varphi_{X,Y}\varphi_X = \varphi_{X,Y}$, $\varphi_X\varphi_{Y,X} = \varphi_{Y,X}$, and $\varphi_{Y,X}\varphi_{X,Y} = \varphi_X$.*

Proof. We let the inclusion map $i_Y: M \rightarrow Y$ be $i_Y \stackrel{\text{def}}{=} \varphi_{X,Y}i_X$, and similarly we define the projection $p_Y \stackrel{\text{def}}{=} p_X\varphi_{Y,X}$. Conversely, given inclusion and projection maps to Y , we let $\varphi_{X,Y} = i_Y p_X$ and $\varphi_{Y,X} = i_X p_Y$. The reader may verify that this works. \square

Thus, if we know what the transition maps $\varphi_{X,Y}$ are explicitly, then we may augment our presentation by adding new maps i_Y and p_Y , and relations as in the claim above and its proof. Having such an augmentation will make it more obvious that M is a summand of both Y and X . The point is that the data of the transition maps is data which is entirely defined in terms of morphisms in \mathcal{C} , not in any completion thereof.

Rewriting φ_X as $\varphi_{X,X}$ may make the statement more intuitive. We now generalize this to the form we will use, and leave proofs to the reader.

Claim 2.11. *Suppose that we have a nonempty collection $\{X_\alpha\}$ of objects in \mathcal{C} for which M is a summand (that is, with each object we fix an inclusion and projection map defining M as a summand). Let $\varphi_{\alpha,\beta}$ be the map $X_\alpha \rightarrow X_\beta$ given by the composition $X_\alpha \rightarrow M \rightarrow X_\beta$ of a projection map with an inclusion map. Note that this implies $\varphi_{\beta,\gamma}\varphi_{\alpha,\beta} = \varphi_{\alpha,\gamma}$. The maps $\varphi_{\alpha,\beta}$ are morphisms in \mathcal{C} , so let us suppose that we know how to describe these maps explicitly. We may obtain a presentation of $\mathcal{C}(M)$ as follows. The generators will consist of those generators of \mathcal{C} as well as new maps $p_\alpha: X_\alpha \rightarrow M$ and $i_\alpha: M \rightarrow X_\alpha$. The relations will consist of those relations in \mathcal{C} as well as the new relations $i_\beta p_\alpha = \varphi_{\alpha,\beta}$ and $p_\alpha i_\alpha = \mathbb{1}_M$.*

Claim 2.12. *A collection of functions $\varphi_{\alpha,\beta}: X_\alpha \rightarrow X_\beta$ will define a mutual summand if and only if $\varphi_{\beta,\gamma}\varphi_{\alpha,\beta} = \varphi_{\alpha,\gamma}$ for all α, β, γ .*

Definition 2.13. We call a collection of morphisms $\varphi_{\alpha,\beta}$ satisfying $\varphi_{\beta,\gamma}\varphi_{\alpha,\beta} = \varphi_{\alpha,\gamma}$ a *consistent family of projectors*.

Remark 2.14. A similar concept is a *consistent family of isomorphisms*, which occurs when all $\varphi_{\alpha,\beta}$ are isomorphisms. This is the data required to state that a family of objects are canonically isomorphic.

This concludes the discussion of adding numerous projections and inclusions to the presentation of $\mathcal{C}(M)$. Of course, we may want to augment our presentation still further, to help describe other features of the new objects.

Remark 2.15. Given a consistent family of projectors, a map in $\mathcal{C}(M)$ from M to any object Z can be specified by one of the following equivalent pieces of data: for a single X of which M is a summand, a map f from $X \rightarrow Z$ such that $f\varphi_{X,X} = f$; a “consistent” family of maps $f_\alpha: X_\alpha \rightarrow Z$ such that $f_\alpha\varphi_{\beta,\alpha} = f_\beta$. We will usually define a map by using one member of the consistent family, but once the map is defined, we will freely use any member of the family (and will often investigate what certain other members of the family look like).

The goal of the next chapter is to present \mathcal{B}_{gBS} by generators and relations. We know that, for any parabolic subgroup J , B_J will be a summand of $B_{\underline{i}}$ where \underline{i} is any reduced expression for w_J . For instance, $B_{s_1s_2s_1s_3s_2s_1}$ is a summand of $B_{s_1} \otimes B_{s_2} \otimes B_{s_1} \otimes B_{s_3} \otimes B_{s_2} \otimes B_{s_1}$. The set of reduced expressions for w_J gives a family of objects in \mathcal{B}_{BS} for which we wish to have inclusion and projection maps, which means that we will need to find an explicit description of a consistent family of projectors $\varphi_{\underline{i},\underline{j}}: B_{\underline{i}} \rightarrow B_{\underline{j}}$ for any two reduced expressions of w_J . Finding these maps and proving that they form a consistent family will require some knowledge of the expression graph for w_J , which we provide in the next section. The subsequent sections will define these maps and prove that they pick out the appropriate summand B_J , and will use this to define a diagrammatic presentation for \mathcal{B}_{gBS} . Finally, we will augment this presentation to describe more easily the isomorphisms (2.11), and (2.12).

3. A THICKER CALCULUS

3.1. Expression graphs and path morphisms. The terminology of this section is ad hoc, and not standard. This is due to ignorance, not malice.

Notation 3.1. Let w be an element of S_n . Let $\widetilde{\Gamma}_w$ be the (finite) set of reduced expressions for w . We give $\widetilde{\Gamma}_w$ the structure of an undirected graph by placing an edge between x and y if and only if they are related by a single application of either $s_i s_j s_i = s_j s_i s_j$ for i, j adjacent, or $s_i s_j = s_j s_i$ for i, j distant. We may distinguish between these two different kinds of edges, calling the former *adjacent edges* and the latter *distant edges*. Let Γ_w be the graph which is the quotient of $\widetilde{\Gamma}_w$ by all distant edges; that is, one identifies any two vertices connected by a distant edge, and removes the distant edges. To simplify things, we will often write a reduced expression as a sequence of indices; for instance, 121 or 1, 2, 1 for $s_1 s_2 s_1$. We call $\widetilde{\Gamma}_w$ the *expanded expression graph* and Γ_w the *(conflated) expression graph*. We may place an orientation on the expression graph, or on the adjacent edges of the expanded expression graph, using the *lexicographic partial order*, so that arrows always go from $i, i+1, i$ to $i+1, i, i+1$. When we speak of an *oriented path* in $\widetilde{\Gamma}$, we refer to a path which may follow distant edges freely, but can only follow adjacent edges along the orientation. A *reverse oriented path*

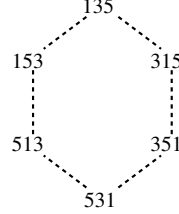
is an oriented path backwards. When we say *path* with no specification, we refer to any path, which may follow the adjacent edges in either direction.

Example 3.2. The expanded expression graph for 21232 in S_4 .

$$12312 \cdots 12132 \longrightarrow 21232 \longrightarrow 21323 \cdots 23123$$

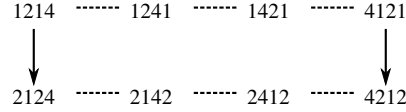
The following examples will include some important definitions.

Example 3.3. The expanded expression graph for 135 in S_6 .



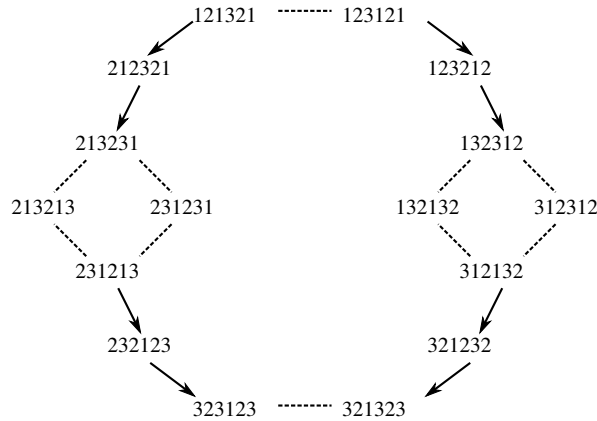
There are two distinct paths from 135 to 531, which form a hexagon. We refer to any cycle of this form appearing in any expanded expression graph (which will occur whenever $\dots ijk \dots$ occurs inside a larger word, for i, j, k all mutually distant) as a *distant hexagon*.

Example 3.4. The expanded expression graph for 1214 in S_5 .



There are two distinct (oriented) paths from 1214 to 4212, which form an octagon. As above, we refer to any cycle of this form in any expanded expression graph as a *distant octagon*.

Example 3.5. The expanded expression graph for the longest element 121321 in S_4 .



There are different kinds of cycles appearing here. For instance, a square is formed between 213231 and 231213, because there are two *disjoint* distant moves which can be applied, and one can apply them in either order. Any square of this kind in any graph we call a *disjoint square* (the edges may be either distant or adjacent edges, for instance

121343 \rightarrow 212434). Ignoring the ambiguities created by the two disjoint squares in this picture, there are two oriented paths from 121321 to 323123. We refer to any cycle of this form in any expanded expression graph as a *Zamolodchikov cycle*.

Expression graphs were studied deeply in Manin-Schechtman [10]. In that paper they define an n -category, where one can at various stages view expressions as objects, distant and adjacent edges as morphisms between objects, the cycles above as 2-morphisms between morphisms, and on to even higher structure. We will use only a few of their results here.

Remark 3.6. To the casual reader, it may not be obvious how Manin-Schechtman discusses expression graphs at all, or how the results there translate into the results here. We recommend closely reading Chapter 2 of that paper just for the example of $I = \{1, \dots, n\}$ and $k \leq 4$, and skimming Chapter 3, always keeping the examples of S_3 (see Chapter 3 Example 6) and S_4 in mind. The key results will be Chapter 2 Theorem 3 and Lemma/Corollary 8, which we will translate below.

Proposition 3.7. *For any $w \in S_n$, the graph $\widetilde{\Gamma}$ is connected. The 4 types of cycles mentioned above (disjoint squares, distant hexagons, distant octagons, and Zamolodchikov cycles) generate $H^1(\widetilde{\Gamma})$ topologically. Viewing these cycles as transformations on oriented paths (switching locally from one oriented path in a cycle to the other), any two oriented paths with the same source and target can be reached from each other by these cycles.*

The same statements are true for Γ , restricting oneself only to disjoint squares and Zamolodchikov cycles (for the remaining cycles are trivial in Γ).

Proof. See Manin-Schechtman Chapter 2 Corollary 8. □

Now we see how to combine the theory of expression graphs with morphisms in \mathcal{B}_{BS} .

Definition 3.8. To a vertex $x \in \widetilde{\Gamma}_w$ we may associate an object $B_x \in \mathcal{B}_{\text{BS}}$, which is simply $B_{i_1} \otimes \dots \otimes B_{i_d}$ when $x = s_{\underline{i}}$. To a path $x \rightsquigarrow y$ in $\widetilde{\Gamma}_w$ we may associate a morphism $B_x \rightarrow B_y$, by assigning the 4-valent vertex to a distant edge, and the 6-valent vertex to an adjacent edge. We call this the *path morphism* associated to the path. To a length 0 path at vertex x we associate the identity morphism of B_x . Note that the reversing the direction of a path will correspond to placing the path morphism upside-down.

Proposition 3.9. *Let f and g represent two oriented (resp. reverse oriented) paths from x to y . Then their path morphisms are equal.*

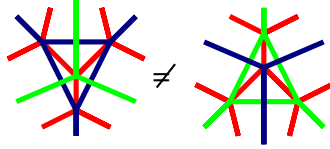
Proof. Since oriented paths f and g are related by the various cycle transformations above (in Proposition 3.7) we need only show that the path morphism is unchanged under these cycle transformations. Because \mathcal{B}_{BS} is a monoidal category, the morphisms associated to either path in a disjoint square are equal. Relation (2.24) is a restatement of the fact that the morphisms associated to either path in the distant hexagon are equal; similarly for (2.23) and the distant octagon. Relation (2.30) is a restatement of

the fact that the morphisms associated to either *oriented* path in the Zamolodchikov cycle are the same. Flipping the pictures upside-down yields the statement for reverse oriented paths. There is one additional kind of loop which is possible for oriented paths: following a distant edge from x to y and then right back to x . But this is the identity by (2.19). \square

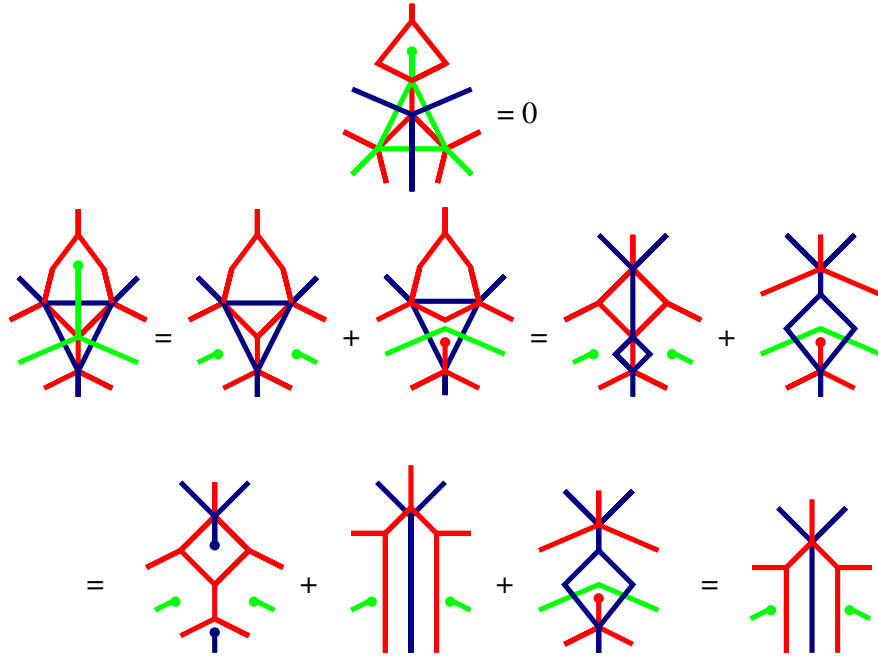
Remark 3.10. Caveat the First: if x and y are connected by a distant edge, then the loop $B_x \rightarrow B_y \rightarrow B_x$ is the identity of B_x , while if the edge is an adjacent edge then the loop is *not* the identity, but is instead the *doubled 6-valent vertex*, an idempotent of B_x . In this sense adjacent edges and distant edges are unsurprisingly different.

Remark 3.11. Caveat the Second: the only cycle where the assumption “oriented or reverse oriented” mattered was the Zamolodchikov cycle, for disjoint cycles are trivial, hexagon cycles are always oriented, and octagon cycles are always either oriented or reverse oriented. However, surprisingly, the orientation assumption is *entirely necessary* for the Zamolodchikov cycle!

For instance, consider the two possible (necessarily unoriented) path morphisms from 212321 to 321232, as pictured below (seen as morphisms fitting in a circle with boundary 212321232123).



To show that they are non-equal, we attach an aborted 6-valent vertex to the top of both sides: the right is clearly zero by (2.33), while the left is nonzero.



In this calculation, the first equality comes from (2.25), the second from (2.27) and (2.29), the third from (2.26), and the fourth from (2.33).

Corollary 3.12. *Consider a set of vertices $\{x_\alpha\}$ which are connected using only distant edges, and let $\varphi_{\alpha,\beta}$ be the (unique) path morphism (using only distant edges) from B_{x_α} to B_{x_β} . Then φ forms a consistent family of isomorphisms.*

Proof. Because the paths use only distant edges, they are oriented, and their compositions are also oriented. The previous proposition therefore immediately implies that $\varphi_{\beta,\gamma}\varphi_{\alpha,\beta} = \varphi_{\alpha,\gamma}$. They are isomorphisms since $\varphi_{\alpha,\alpha}$ is the identity map. \square

The 4-valent vertices/distant edges are all isomorphisms and do not play a significant role. Henceforth, whenever we speak of the *length* of a path in Γ_w or $\widetilde{\Gamma}_w$ we mean the number of adjacent edges in the path.

Definition 3.13. We abuse notation henceforth in order to talk about path morphisms of Γ . To a vertex $x \in \Gamma$ we may associate a class of objects, one for each vertex in $\widetilde{\Gamma}$ above x , with a fixed family of transition isomorphisms between them. To a path $x \rightsquigarrow y$ in Γ , we may associate its *path morphism*, by which we may refer to either the family of morphisms from some lift of x to some lift of y given by some lift of the path, or some specific element of this family. See Remark 2.15.

3.2. The longest element. We begin to study the longest element $w \in S_n$ in detail, using further results from Manin-Schechtman. Because reduced expressions of elements do not change when one includes them from a parabolic subgroup into the whole group, we may rephrase the results for any w_J , the longest element in the parabolic subgroup determined by a *connected* sub-Dynkin diagram $J = \{i, i+1, \dots, j\}$. Unless otherwise stated, Γ and $\widetilde{\Gamma}$ refer to the expression graphs of w_J , and all parabolic subsets are connected.

Notation 3.14. For $x, y \in \Gamma$, we write $x \downarrow y$ for the oriented length 1 path from x to y , $y \uparrow x$ for the reverse path, $x \searrow y$ for an oriented path from x to y of unspecified length, $y \nearrow x$ for a reverse path. If $x \downarrow y$ then the path is unique, while if $x \searrow y$ then there may be multiple paths; only the path morphism is unique. We denote the unique path morphism $\psi_{x \searrow y}$. There is also a unique map $\psi_{y \nearrow x}$ coming from the reverse path.

Proposition 3.15. *There is a unique source s_J in Γ , and a unique sink t_J . Let m be the length of the shortest (not necessarily oriented) path from s_J to t_J . Then every vertex lies on some oriented path $s_J \searrow t_J$ of length m , and every oriented path $x \searrow y$ can be extended to a length m path $s_J \searrow x \searrow y \searrow t_J$.*

Proof. See Manin-Schechtman Chapter 2 Theorem 3. \square

Remark 3.16. It is easy to see what s_I and t_I are: we give a representative vertex in $\widetilde{\Gamma}$ for the vertex in Γ . Suppose that $I = \{1, 2, \dots, n\}$. Then when $n = 1, s = 1$; $n = 2, s = 121$; $n = 3, s = 121321$; $n = 4, s = 1213214321$; $n = 5, s = 121321432154321$. At each stage we add a new sequence $n, n-1, \dots, 1$. Similarly, when $n = 3, t = 323123$;

$n = 4, t = 434234\underline{1234}$; $n = 5, t = 5453452345\underline{12345}$. The reader should be able to see the pattern.

Remark 3.17. Here and elsewhere, we will be illustrating various proofs and definitions by using examples. This is a dangerous practice, but we solemnly promise that the general case truly will be evident to the reader after a brief study of the examples. We will be drawing path morphisms soon enough, and it is incredibly inconvenient to draw a general case; while the general case could be made explicit symbolically, the advantage of graphical calculus is lost when one passes to long strings of symbols. The examples we give will be more enlightening.

Since it will be general enough to do the longest element w in S_n itself, we state which example we do by specifying n , and letting $I = \{1, \dots, n\}$. For general statements we usually use the letter J , or will omit the labelling entirely.

While it might seem as though one reduced expression of w_J is as good as any other, the fact that orientation matters, witnessed in Remark 3.11, really does make s_J and t_J into special vertices, to which we shall now devote many pages.

Notation 3.18. (Example: $n = 5$) We now fix notation for several useful vertices in $\tilde{\Gamma}$ lying over s_I and t_I . We write s_I^R for the default sequence, which is given as above, 121321432154321. Note that $s_I^R = s_K^R 54321$ for $K = \{1, 2, 3, 4\}$. We write s_I^L for the horizontal flip of the default sequence, also thought of as the “left-facing” default sequence, 123451234123121 = 12345 s_K^L . Now we look for expressions somewhere between these two. Let $i \in I$, and let $M_i = \{1, 2, \dots, i\}$. Then we write $s_{I,i}^R$ for the sequence that begins as s_I^L until $i + 1$, i.e. with 123451234...12... $i + 1$ and then concludes with $s_{M_i}^R$. Explicitly, $s_{I,5}^R = s_I^R$, $s_{I,4}^R = 12345 \ 1213214321$, $s_{I,3}^R = 123451234 \ 121321$, $s_{I,2}^R = 123451234123 \ 121$ and $s_{I,1}^R = s_I^L$. Flipping all of these horizontally, we get $s_{I,i}^L$. When I is understood, we often leave it out of the notation. Also, we will primarily investigate the “right-handed” results (all the “left-handed” results follow by a horizontal flip) so when the superscript is omitted we assume it is R .

Similarly, let $t^R = 545345234512345 = t_1^R, t_2^R = 54321 \ 5453452345$, and so forth, with t^L being the horizontal flips. Here, we think of M_i as being $\{i, i + 1, \dots, n\}$.

The salient feature of $s_{I,i}^R$ is that, coming from the right, it counts from 1 up to i , and continues to give a presentation for the longest element of $M_i = \{1, 2, \dots, i\}$. We will see that when B_{s_I} interacts with other colors on the right, and those other colors are in M_i , then $s_{I,i}^R$ is the most useful representative of the isomorphism class, because the parts on the left (123451234 when $i = 3$) will not play an important role. This will become clear in examples to come. A similar statement holds for t_I , with $M_i = \{i, \dots, n\}$.

Now we define our object of study.

Definition 3.19. Let z_J denote the unique path morphism from $s_J \searrow t_J$.

Our eventual goal is to show that z_J is one member of a consistent family of projectors, corresponding to B_J as a summand of B_x for any $x \in \Gamma$. The morphism z_J can be made

to factor through any object B_x , because some oriented path goes through x , which is already a motivating reason to investigate z_J . Before we can prove the key result, we will need to perform many calculations first, and it will be useful to examine some specific paths from s_J to t_J , whose path morphisms can be chosen as representatives for z_J .

Notation 3.20. First, we introduce a useful subpath. For $i < j$ let $F = F_{i,j}$ denote the “flip” path, defined by example here: $F_{1,4} = 1234321 \downarrow 1243421 = 4123214 \downarrow 4132314 = 4312134 \downarrow 4321234$, $f_{3,5} = 34543 \downarrow 35453 = 53435 \downarrow 54345$. In general, $F_{i,j}$ starts at the sequence going from i up to j and back down to i , and repeatedly applies an adjacent edge to the middle until the final expression is reached. We will usually just call the flip map F when the indices are understood, and also use the same notation F for the opposite path to this one. The flip path F can also be viewed as the unique oriented path from source to sink in Γ_v for v the appropriate permutation. Here is the path morphism for $F_{1,5}$.

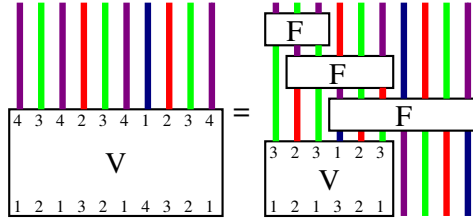


Notation 3.21. Next, we inductively define a specific path V_J^R from $s_J^R \searrow t_J^R$. When J consists of a single index $s_J = t_J$ and the path is trivial. Suppose we have defined V_K^R for all $K \subset J$.

(Example: $n = 5$) Let us define V_I^R by example. Let $K = \{1, 2, 3, 4\}$. Then $s_I^R = s_K^R 54321$. To obtain V_I^R , first we apply V_K^R to get $t_K^R 54321 = 434234123454321$, and then we apply a sequence of flip maps of decreasing size $434234123454321 \searrow 434234543212345 \searrow 434543234512345 \searrow 454345234512345 \searrow 545345234512345 = t_I^R$.

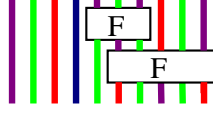
The path V_J^L is the horizontal flip of this.

Example 3.22. (Example: $n = 4$) Here is the picture of V_I :



Notation 3.23. (Example: $n = 4$) These sequences of flips at the top of the picture (or at the end of the path V_I) will play a key computational role. We call the sequence of flips FR_1 . Let us call attention to one feature of this sequence of flips, explaining this name. There is a single instance of the index 1 in t_I^R (i.e. a single blue line on top), and if we wish to bring the index 1 to the far right using only flip maps, then one must do it with the sequence of flip maps as in V_I . Suppose instead that one wanted to bring the index 2 to the far right. One can start instead with $t_{I,2}^R = 4321434234 = 4321t_{M_2}^R$

for $M_2 = \{2, 3, 4\}$ on top. Then, the sequence of flips at the end of V_{M_2} would bring 2 to the far right. We call this sequence of flips FR_2 , as pictured below.



Similarly, to bring 3 to the right, we start with $t_{I,3}^R$ and apply the flips from V_{M_3} , and so forth. To bring 4 to the right, one needn't do a thing, so FR_4 is the trivial path. Note the unfortunate way things are phrased above: since morphisms go from bottom to top in a picture, FR_i is really bringing i from the right to its final resting place in t_i^R , not vice versa. However, we also denote the vertical flip of this map by FR_i , which now is a map from $t_i^R \nearrow x$ for some expression x having i on the right.

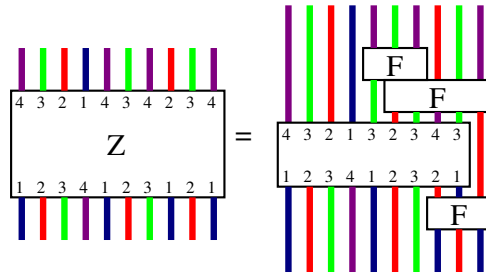
To be very precise, we are using FR_i to denote an oriented path in Γ , *not* a path morphism or a path in $\tilde{\Gamma}$, so that if we want to apply FR_3 as a path morphism to t_I^R we must first apply the appropriate distant edges to reach $t_{I,3}^R$, and then apply the sequence of flip pictures. However, as usual, we will abuse notation and speak of FR_i as though it were a morphism in \mathcal{B}_{BS} .

Similarly, we may apply a sequence of flips to s_I to bring an index to the right. The most complicated set of flips is now FR_4 , which sends $\underline{1213214321} \searrow \underline{2123214321} \searrow \underline{2321234321} \searrow \underline{2324321234}$ (take the above picture, flip it upside-down, and change the colors), while the simplest is now FR_1 , which is the identity map. We use FR_i to denote the appropriate sequence of flips, regardless of whether we start or end at s_K or t_K . However, we do *not* make a definition of FR_i for an arbitrary vertex in Γ , only for s_I and t_I .

As usual, FL_i denotes the horizontal flip of the above.

Claim 3.24. *Fix arbitrary $i \in J \subset I$. There is an oriented path $s_J \searrow x \searrow y \searrow t_J$ such that the path $s_J \searrow x$ is FR_i (so that x has i on the right), the path $t_J \nearrow y$ is FR_i (so that y also has i on the right), and the path $x \searrow y$ does not alter the rightmost index i at all.*

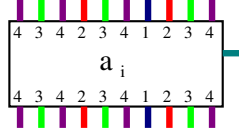
Example 3.25. (Example: $n = 4$) When $i = 2$, we have



where the unlabeled box represents some unspecified oriented path.

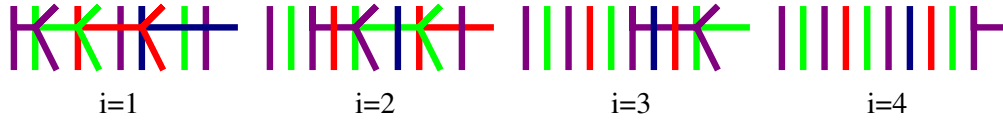
Proof. This follows from Manin-Schechtman theory (the existence of sources and sinks) when applied to the expression graph for $w_J s_i$. We leave the proof as an exercise to the reader. \square

3.3. Thick trivalent vertices and flip maps. Because $B_J \otimes B_i \cong B_J\{1\} \oplus B_J\{-1\}$ for $i \in J$, there should be some projection/inclusion maps between $B_J \otimes B_i$ and B_J of degree ± 1 . When $J = \{i\}$ so that $B_J = B_i$, we know that the maps of degree -1 are drawn as a trivalent vertex. Whatever they are for B_J , we should think of them as a *thick trivalent vertex*, merging two copies of B_J and spitting out a third i -colored strand. To specify this map, once we have the consistent family of projectors corresponding to B_J , we need only give this map when pre- and post-composed with the inclusion/projection from B_J to B_{t_J} (or B_{s_J}). So we seek some morphism of degree -1 of the following form (drawn here for $n = 4$ and for t_J^R):

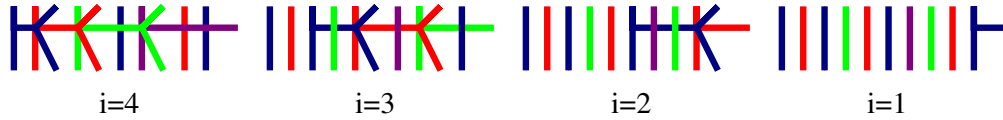


Teal represents the arbitrary index $i \in J$. We shall define this morphism soon, and name it $a_{t_J^R, i}^R$. Similarly, since $B_i \otimes B_J$ also splits into two copies of B_J , there should be a thick trivalent vertex on the left as well, $a_{t_J^L, i}^L$. For these maps, t_J and i can be determined from the colors on the boundary, and R or L determined by where the additional teal line sticks out, so we will often call it simply a_i or a . Similarly, there should be maps a_i from s_J as well. As for the iterated flip maps of the previous section, we do not define maps a_i for an arbitrary reduced expression of w_J , only for s_J and t_J .

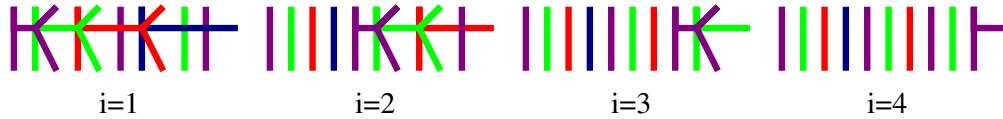
Definition 3.26. (Example: $n = 4$) Let the morphism $a_i = a_{t_I^R, i}^R$ be the morphism described in the following examples. It has top and bottom boundary t_I^R and side boundary i .



Similarly, one can define $a_i = a_{s_I^R, i}^R$ as follows.



Remark 3.27. (Example: $n = 4$) In analogy to the maps FR_i above for t_I , the case of $i = 1$ is the most complicated, and $i = n$ the least complicated (the opposite is so for s_I). Note further that for $i > 1$, certain of the lines can be pulled harmlessly to the left, leading to the expression $t_{I, i}^R$ for t_I . Rewriting the maps a_i so that they have top and bottom boundary $t_{I, i}$, they have a more intuitive form.



This is simply $a_{M_i, i}$ with extra lines to the left, where $M_i = \{i, \dots, n\}$.

Remark 3.28. Note that a_i can also be defined inductively. For instance, $a_{s_I^R, i}^R$ is a single 6-valent vertex to the right of $a_{s_K^R, i-1}$ for $K = \{1, \dots, n-1\}$. This may help to understand the general case or the induction step of many of the proofs below.

Now it is time to gather some results about the various maps a_i, FR_i, z . Almost every result has an equivalent version with the colors switched (i.e. switching s_J and t_J) or flipped horizontally (i.e. switching L and R). The key relation, which leads to all the others, is the following:

Claim 3.29. (*Example: $n = 5$*) We have the following equality.

$$(3.1) \quad \begin{array}{c} \text{Diagram with 5 vertical lines (blue, red, green, purple, black) and a box labeled } F \text{ with top labels } 1, 2, 3, 4, 5, 4, 3, 2, 1 \text{ and bottom labels } 5, 4, 3, 2, 1, 2, 3, 4, 5. \end{array} = \begin{array}{c} \text{Diagram with 5 vertical lines and a box labeled } F \text{ with top labels } 1, 2, 3, 4, 5, 4, 3, 2, 1 \text{ and bottom labels } 5, 4, 3, 2, 1, 2, 3, 4, 5. \end{array} \cdot$$

Proof. Writing out the flip map in full, this is an immediate application of relation (2.29). Explicitly,

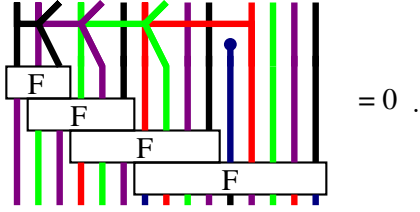
$$\begin{array}{c} \text{Diagram with 5 vertical lines and a box labeled } F \text{ with top labels } 1, 2, 3, 4, 5, 4, 3, 2, 1 \text{ and bottom labels } 5, 4, 3, 2, 1, 2, 3, 4, 5. \end{array} = \begin{array}{c} \text{Diagram with 5 vertical lines and a box labeled } F \text{ with top labels } 1, 2, 3, 4, 5, 4, 3, 2, 1 \text{ and bottom labels } 5, 4, 3, 2, 1, 2, 3, 4, 5. \end{array} = \begin{array}{c} \text{Diagram with 5 vertical lines and a box labeled } F \text{ with top labels } 1, 2, 3, 4, 5, 4, 3, 2, 1 \text{ and bottom labels } 5, 4, 3, 2, 1, 2, 3, 4, 5. \end{array} = \begin{array}{c} \text{Diagram with 5 vertical lines and a box labeled } F \text{ with top labels } 1, 2, 3, 4, 5, 4, 3, 2, 1 \text{ and bottom labels } 5, 4, 3, 2, 1, 2, 3, 4, 5. \end{array}$$

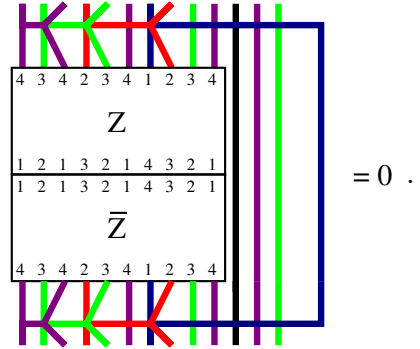
The box labelled F in the intermediate calculations is the flip map for $\{2, 3, 4, 5\}$. \square

Claim 3.30. We have the following equalities, which are effectively properties of the most complicated map a_1 for t_I . The first two are examples of the general equation for $n = 4$, the latter two for $n = 5$.

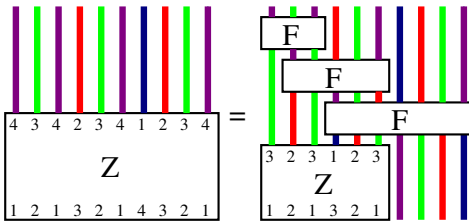
$$(3.2) \quad \begin{array}{c} \text{Diagram with 4 vertical lines and three boxes labeled } F \text{ with top labels } 1, 2, 3, 4, 3, 2, 1 \text{ and bottom labels } 4, 3, 2, 1, 3, 2, 4. \end{array} = \begin{array}{c} \text{Diagram with 4 vertical lines and three boxes labeled } F \text{ with top labels } 1, 2, 3, 4, 3, 2, 1 \text{ and bottom labels } 4, 3, 2, 1, 3, 2, 4. \end{array} \cdot$$

$$(3.3) \quad \begin{array}{c} \text{Diagram with 5 vertical lines and a box labeled } Z \text{ with top labels } 4, 3, 4, 2, 3, 4, 1, 2, 3, 4 \text{ and bottom labels } 1, 2, 1, 3, 2, 1, 4, 3, 2, 1. \end{array} = \begin{array}{c} \text{Diagram with 5 vertical lines and a box labeled } Z \text{ with top labels } 4, 3, 4, 2, 3, 4, 1, 2, 3, 4 \text{ and bottom labels } 1, 2, 1, 3, 2, 1, 4, 3, 2, 1. \end{array} \cdot$$

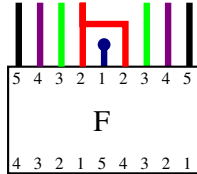
(3.4)  = 0 .

(3.5)  = 0 .

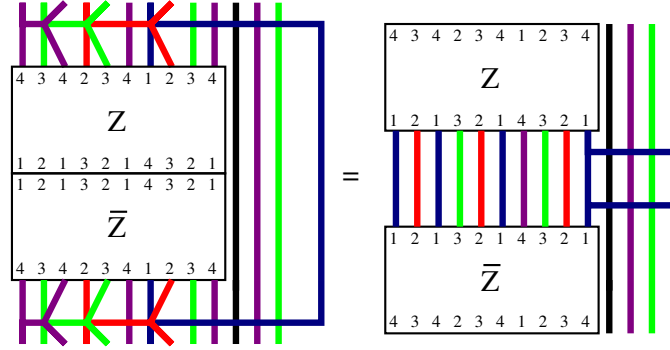
Proof. The first equality is easily seen to be an iterated use of (3.1), starting with the leftmost flip and moving to the right. To get the second equality, remember that we can always express z_I as

(3.6)  = 0 .

using the path V_I . Placing $z_{\{1,2,3\}}$ below (3.2) yields (3.3). Applying (3.2) to all but the last flip in (3.4), the diagram factors through the following picture as it enters the final flip:



However, the first thing that happens in a flip is a 6-valent vertex, which kills the aborted 6-valent vertex by (2.33). Finally, to show (3.5), we may apply (3.3) to both the top and bottom, obtaining



This is 0 by (2.16). □

It may be useful for the reader to work through the examples of $n = 2, 3$ explicitly, writing out flip maps and z in full and checking these results. The general computations are no more difficult. One should think of the picture on top of (3.4) (ignoring the flips) as being an “aborted” version of a_1 .

Now we generalize these results to derive facts about a_i for any i .

Claim 3.31. *We have the following equalities, for any $i \in I$ (and which all have t_I^R as the top boundary). Here, \bar{z} represents z upside-down.*

$$(3.7) \quad \begin{array}{|c|} \hline a_i \\ \hline FR_i \\ \hline \end{array} = \begin{array}{|c|} \hline FR_i \\ \hline \end{array}.$$

$$(3.8) \quad \begin{array}{|c|} \hline a_i \\ \hline \begin{array}{|c|} \hline 4 \ 3 \ 4 \ 2 \ 3 \ 4 \ 1 \ 2 \ 3 \ 4 \\ \hline Z \\ \hline 1 \ 2 \ 1 \ 3 \ 2 \ 1 \ 4 \ 3 \ 2 \ 1 \\ \hline \end{array} \\ \hline \end{array} = \begin{array}{|c|} \hline \begin{array}{|c|} \hline 4 \ 3 \ 4 \ 2 \ 3 \ 4 \ 1 \ 2 \ 3 \ 4 \\ \hline Z \\ \hline 1 \ 2 \ 1 \ 3 \ 2 \ 1 \ 4 \ 3 \ 2 \ 1 \\ \hline \end{array} \\ \hline a_i \\ \hline \end{array}.$$

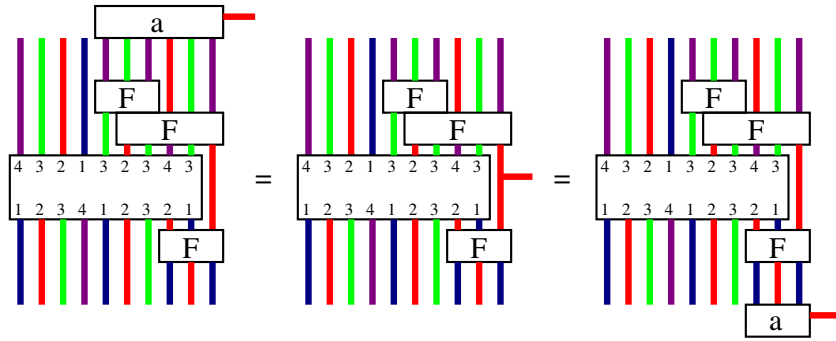
$$(3.9) \quad \begin{array}{|c|} \hline a_i \\ \hline Z \\ \hline \bar{Z} \\ \hline \end{array} = \begin{array}{|c|} \hline Z \\ \hline \bar{Z} \\ \hline a_i \\ \hline \end{array}.$$

$$(3.10) \quad \begin{array}{|c|} \hline a_i \\ \hline a_i \\ \hline Z \\ \hline \end{array} = \begin{array}{|c|} \hline a_i \\ \hline Z \\ \hline \end{array}.$$

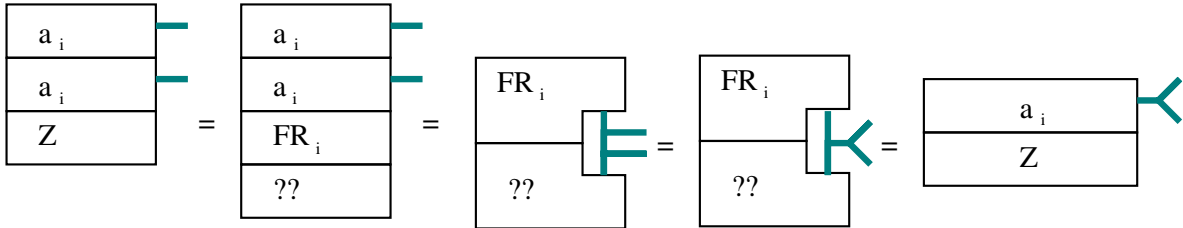
$$(3.11) \quad \begin{array}{|c|} \hline a_i \\ \hline Z \\ \hline \bar{Z} \\ \hline a_i \\ \hline \end{array} \quad \Bigg| = 0.$$

Proof. To prove (3.7), note that for both a_i and FR_i there are extraneous lines which can be harmlessly pushed to the left. In other words, we may as well assume that the top boundary is $t_{I,i}^R$ instead, that the leftmost indices are merely involved in the identity map, and that on the right side we have the exact same equation (3.7) for the special case of $M_i = \{i, i+1, \dots, n\}$ and a_i . But now this result follows from (3.2).

To prove (3.8), we simply use the path of Claim 3.24 and apply (3.7) twice. We provide an example, for $n = 4$ and $i = 2$.



Applying (3.8) twice, we immediately get (3.9). To obtain (3.10), we again use the path of Claim 3.24, and proceed as follows.

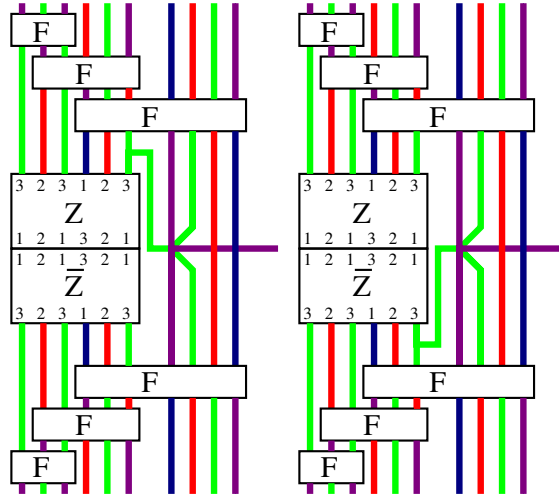


The proof of (3.11) is now basically the same as that of (3.5): use (3.9) to bring the two a_i s together, use (3.10) to combine them, and then use (2.16) to show it is zero. \square

Corollary 3.32. (Example: $n = 4$). We have the following equality, where as usual \bar{z} indicates z upside-down.

The diagram shows an equality between two boxes. Each box has a top edge with the sequence 4 3 4 2 3 4 1 2 3 4 and a bottom edge with the sequence 4 3 4 2 3 4 1 2 3 4. Inside each box, the label Z is above a horizontal line, and \bar{Z} is below it. The horizontal line has the sequence 1 2 1 3 2 1 4 3 2 1 on both sides. Purple lines extend from the top and bottom edges of the boxes.

Proof. This is a special case of (3.9), when $i = n$, but we give another proof anyway for practice. We use (3.22) to rewrite z and \bar{z} . We may then use (3.1) to move the trivalent vertex inwards, and reduce the statement to the following equality:



But this follows immediately from induction. The base case of one color is trivial. \square

Proposition 3.33. (Example: $n = 5$) *The maps of Figure 1 are all zero.*

Proof. This is a generalization of (3.4), dealing with all possible “aborted” versions of a_i . However, this follows almost immediately from (3.4). The first picture of the first row is precisely that of (3.4), while the second picture is what (3.4) would be for $K = \{2, 3, 4, 5\}$ with additional lines 12345 added on the right. Choosing a path $s_I \searrow t_I$ which ends by applying z_K on the left, the map is zero by the K case of (3.4). The third picture in the first row is zero by the $K = \{3, 4, 5\}$ case, and so forth.

For the second row, as for a_2 , we slide 54321 to the left and ignore it. Then, letting $K = \{2, 3, 4, 5\}$, we are left with what would be the first row for (3.33) for K . We leave a more explicit version to the reader. Similarly, for the third row, we slide 543215432 to the left, and what remains is the first row for $K = \{3, 4, 5\}$. The pattern is now clear. \square

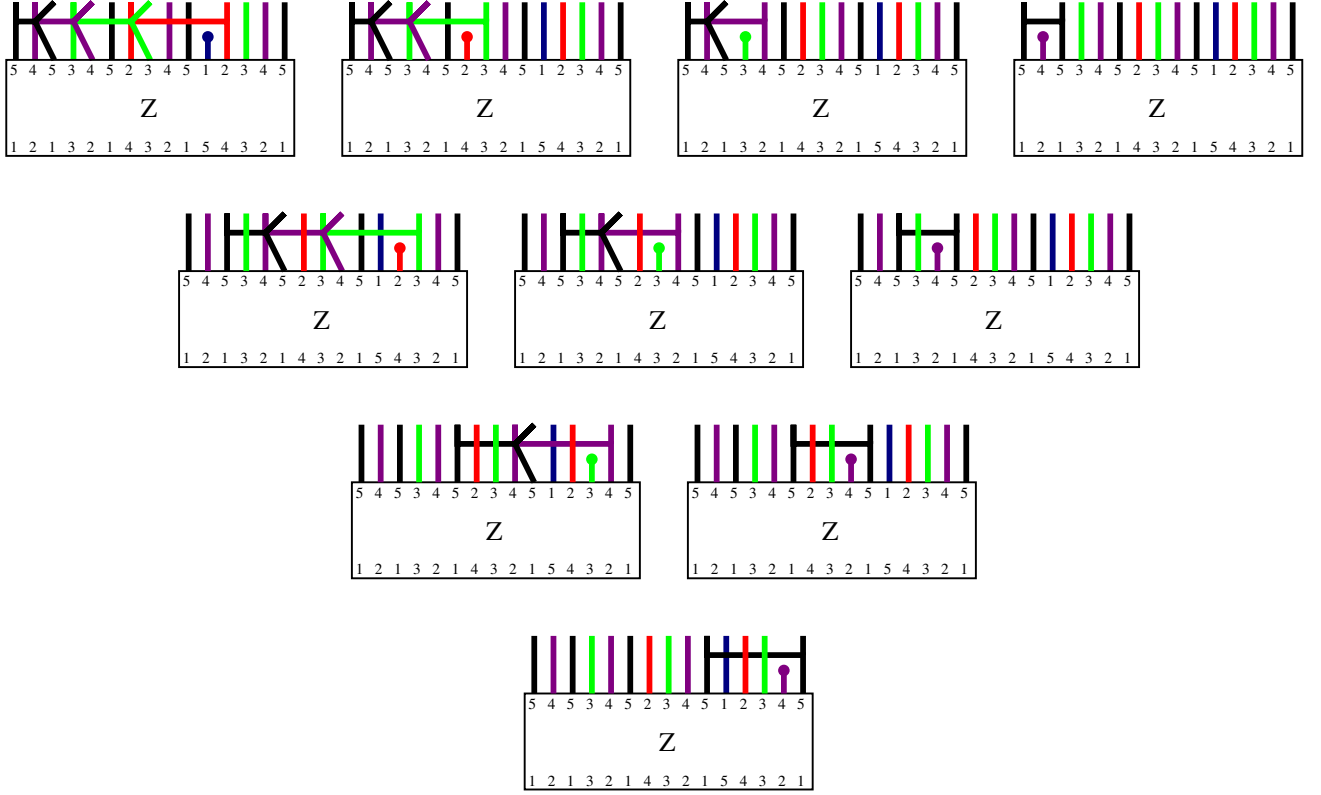


FIGURE 1. The morphisms in Proposition 3.33

We conclude this section with some further properties of a_i . The first one states that (3.10) holds true, even without z_J below. The proof of (3.10) used the existence of z to simplify the proof drastically, while the proof below is an annoying computation. The same statement is true for the other statements here: they are easier to prove when z is placed below them, and we leave these easier proofs as exercises for the reader. In fact, we will only ever care about the maps a_i when they are being post- or pre-composed with z or \bar{z} . Nonetheless, the properties below do hold in the absence of z , so they might as well be proven there.

Proposition 3.34. *The following equations hold, as endomorphisms of (some representative of) either s or t .*

For any $i \in J$:

$$(3.12) \quad \begin{array}{|c|} \hline a_i \\ \hline a_i \\ \hline \end{array} = \begin{array}{|c|} \hline a_i \\ \hline \end{array} \begin{array}{c} \text{---} \\ \text{---} \end{array}$$

For any $i, j \in J$ adjacent:

$$(3.13) \quad \begin{array}{|c|} \hline a_i \\ \hline a_j \\ \hline a_i \\ \hline \end{array} \begin{array}{c} \text{teal line} \\ \text{olive line} \\ \text{teal line} \end{array} = \begin{array}{|c|} \hline a_j \\ \hline a_i \\ \hline a_j \\ \hline \end{array} \begin{array}{c} \text{olive line} \\ \text{teal line} \\ \text{olive line} \end{array}$$

For any $i, j \in J$ distant:

$$(3.14) \quad \begin{array}{|c|} \hline a_i \\ \hline a_j \\ \hline \end{array} \begin{array}{c} \text{teal line} \\ \text{olive line} \end{array} = \begin{array}{|c|} \hline a_j \\ \hline a_i \\ \hline \end{array} \begin{array}{c} \text{olive line} \\ \text{teal line} \end{array}$$

For any $i, j \in J$, with no restrictions ($i = j$ is possible):

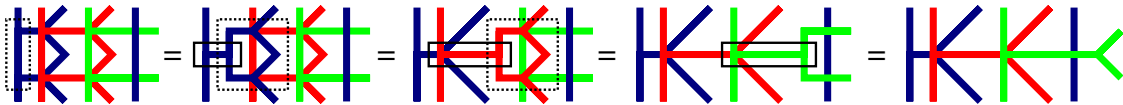
$$(3.15) \quad \begin{array}{|c|} \hline a_i \\ \hline a_j \\ \hline \end{array} \begin{array}{c} \text{teal line} \\ \text{olive line} \end{array} = \begin{array}{|c|} \hline a_j \\ \hline a_i \\ \hline \end{array} \begin{array}{c} \text{olive line} \\ \text{teal line} \end{array}$$

The following equation holds for any $i \in J$ (this does require z below).

$$(3.16) \quad \begin{array}{|c|} \hline a_i \\ \hline Z \\ \hline \end{array} \begin{array}{c} \text{teal line} \\ \text{olive line} \end{array} = \begin{array}{|c|} \hline Z \\ \hline \end{array}$$

We only prove them for s , but the rest is obvious.

Proof of 3.12. This is an application of one-color associativity (2.14), and then repeated uses of two-color associativity (2.29), as illustrated in the following example of 3 colors. The dotted rectangle surrounds that which is to be changed, and the solid rectangle what it becomes; the final step is just a distant slide.



Clearly, any calculation for a_3 reduces to this calculation, regardless of the number of total colors in I , because we may choose a representative $s_{I,3}^R$ of s_I so that this calculation appears on the far right of the diagram. The calculation clearly generalizes to any number of colors. \square

Proof of 3.13. This is an application of one-color associativity (2.14), then two-color associativity (2.27), then repeated uses of three-color associativity (2.30), as illustrated in the following example of 4 colors. The same comments apply as the previous proof.

□

Proof of 3.14. Regardless of which distant colors are chosen, this is a simple application of the distant sliding rules. The reader will observe that any interesting features of a_i will be on strands which are uninteresting in a_j , and vice versa (some strands may be uninteresting for both). This should be clear from the following example.

□

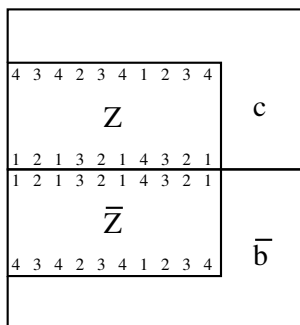
Proof of 3.15. First, it is important to note that the map a_i^R going to the right and the map a_j^L going to the left require *different* choices of representative of s , either s^R or s^L . To make sense of the equation as, say, endomorphisms of s^R , then one must think of a_j^L as first composing by the distant crossings that bring s^R to s^L , applying a_j as normal, and then applying the distant crossings back. As such, this equation can be a pain to write out in general.

Let us do the hardest case: when $i = j = n$ inside $I = \{1, \dots, n\}$. We will demonstrate the example when $n = 5$. Instead of viewing it as an endomorphism of s^R or s^L , we view it as an endomorphism of $121321\underline{4354}23121$ (for the general case, the interesting part in the middle will read $(n-1)(n-2)(n)(n-1)$). Then the reader can observe that the equality may be written suggestively as

This equality follows immediately from three-color associativity (2.30) applied to the dashed box, and distant sliding rules applied to the rest. It should be obvious how this example generalizes to any $n \geq 3$. The cases of $n = 1, 2$ are precisely one-color and two-color associativity.

Proof of 3.16. To prove this, one writes out the map a with a dot, and resolves the dot using (2.25) into a sum of two diagrams. One of the diagrams will die when composed with z , thanks to Proposition 3.33. The other diagram has a dot attached to another 6-valent vertex, so resolves again using (2.25) into a sum of two diagrams. Again, one of the two will die thanks to Proposition 3.33, and so forth. The single surviving diagram is the identity map. The proof of Lemma 3.35 has a similar argument which is made pictorial. \square

Lemma 3.35. (Example: $n = 5$) Let c be one of the pictures in the table of figure 2, and let b be another picture in the same row. For each row, the lines on the right are 54321 except with one index conspicuously absent. The following map is zero, where $z = z_K$ for $K = \{1, 2, 3, 4\}$ and \bar{b} is b upside-down.



Consider the top row; other rows are entirely analogous. Consider what happens when we place a dot on the leftmost picture in various places. Place a dot on the 3rd to left strand on top (the purple strand) and resolve using relation (2.25). You get two diagrams, one of which is the second diagram on the first row, the other of which factors through a map which vanishes when hit with z_K , thanks to Proposition 3.33. If you place a dot instead on the 5th strand (green) and resolve, and ignore diagrams which vanish due to Proposition 3.33, then one is left with the third diagram on the first row. Placing a dot on the 8th strand (red) will give the final diagram on that row. \square

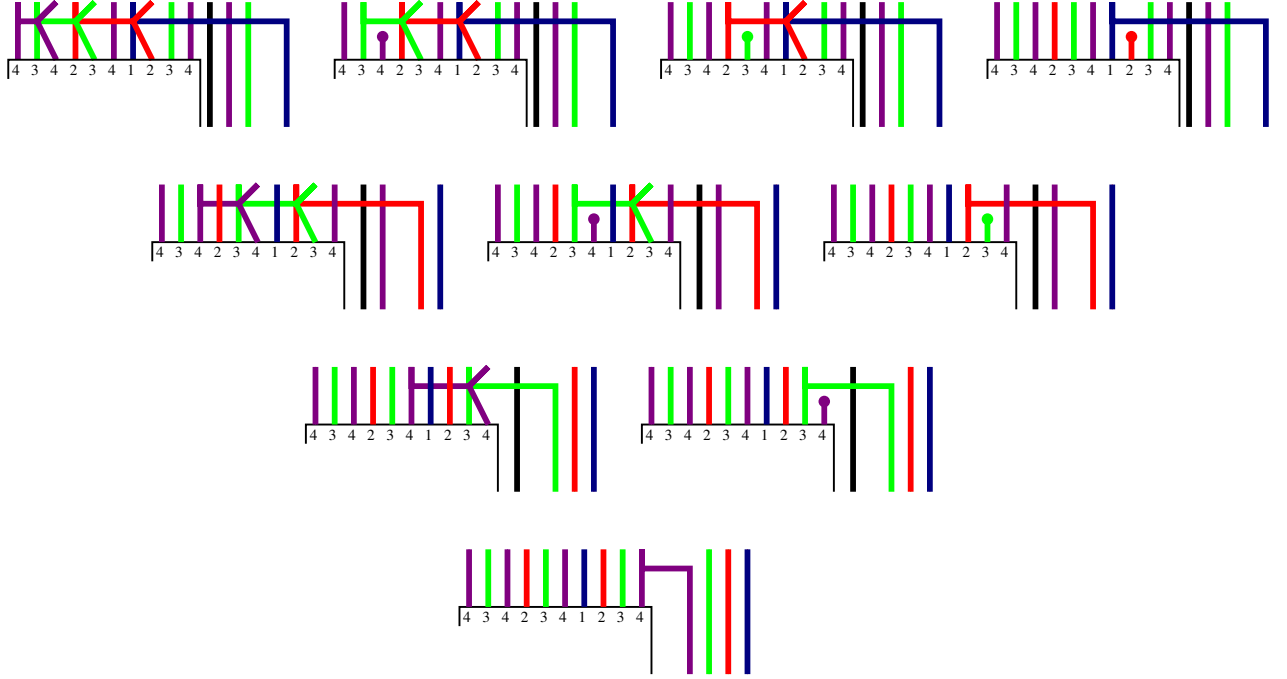
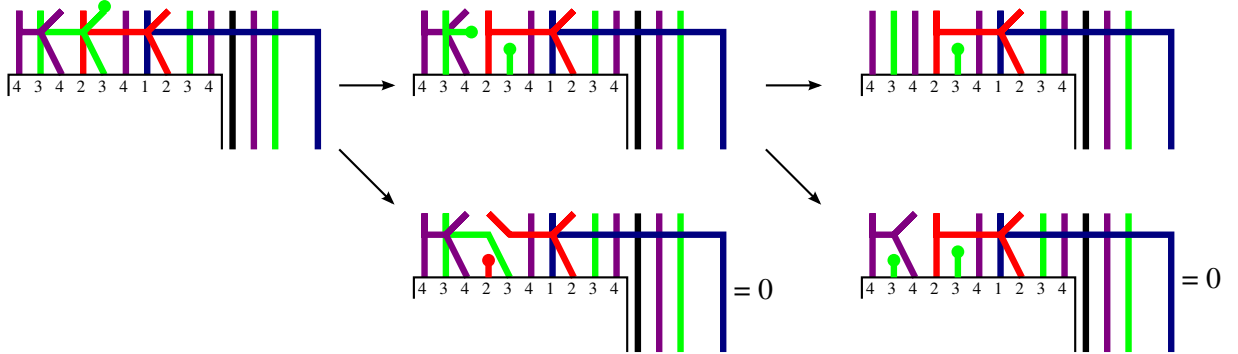


FIGURE 2. Morphisms appearing in Lemmas 3.35 and 3.37

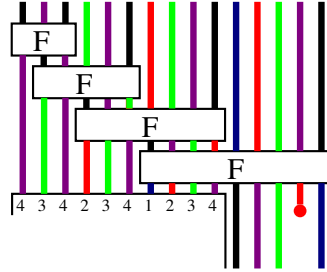
Example 3.36. Placing a dot on the 5th strand and resolving:



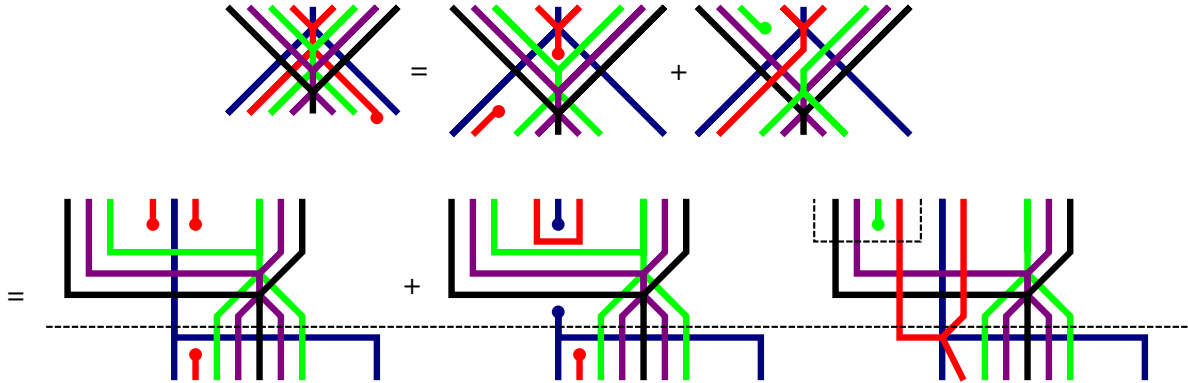
This lemma becomes more significant when viewed in the light of the following two lemmas. Remember that FR_1 is a map from t_I^R to (example: $n = 5$) $434234123454321 = t_K^R 54321$ for $K = \{1, 2, 3, 4\}$.

Lemma 3.37. (Example: $n = 5$) Suppose that we place a dot below FR_i on one of the last strands 54321 , but not on the final strand 1. If we place a dot on strand 2, then the resulting morphism can be rewritten as a linear combination of morphisms which factor through the morphisms on the first row of Figure 2. If we place a dot on strand 3, then it can be rewritten to factor through the second row in that figure. Etcetera.

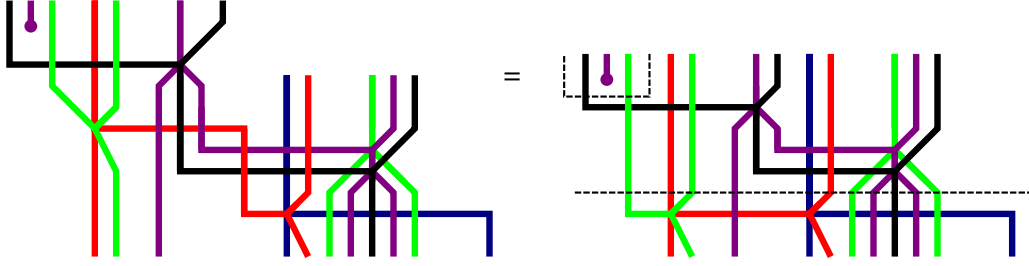
Proof. We shall prove the statement placing a dot on strand 2, and let the reader prove the remainder as an exercise (it follows by the same arguments). The calculation is straightforward but annoying. We are trying to understand the morphism



The first step is to resolve the rightmost flip as below, using (2.25) twice.



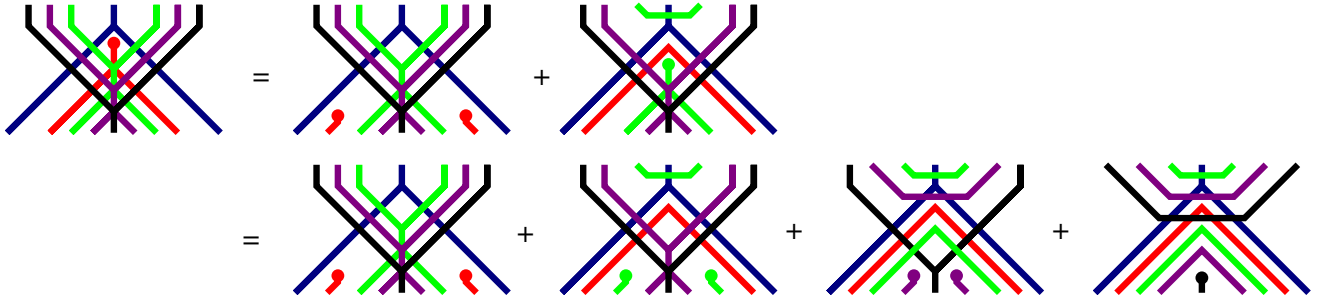
Having written the final three terms suggestively, we see that the regions below the dotted line are familiar. In the first two pictures, the region below the dotted line is precisely the rightmost entry in the first row of Figure 2. Thus we need only deal with the third picture, for which the region below the dotted line is a fragment of the other entries of the first row. In the third picture, the region enclosed by the dotted box will be passed as input to the next flip map in the sequence. The dot coming into the next flip is green, not red, but it is still the 2nd to right input (which will remain true as we iterate this procedure). Therefore we may resolve the next flip map in the same way, to yield two diagrams which factor through the 2nd to right entry of the first row of Figure 2, and a final diagram which has a dot entering the next flip in the 2nd to right input. The third diagram of this iteration is



Once again, the region below the dotted line is a fragment of the next picture in the first row of the figure. We may then repeat the argument, until the final flip map. For the final flip map, we have a dot entering the 6-valent vertex in the middle, yielding morphisms which factor through the trivalent purple vertex, and giving terms which factor through the first entry in the first row of Figure 2. \square

Lemma 3.38. *Suppose that we “abort” FR_i . That is, we follow the path FR_i from t_J up through Γ , but at some vertex x along the way, instead of following the next adjacent edge $x \downarrow y$, we do an aborted 6-valent vertex instead. The resulting morphism then factors through the morphisms in Figure 2, except instead of having a conspicuously absent index on the right, we have a boundary dot instead.*

Example 3.39. Let $n = 5$ and let us abort FR_i at the top of the rightmost flip. We ignore the sequence of lines 434234 appearing on the left of the morphism. Then using (2.25) repeatedly we have



Each term factors through the rightmost entry of some row of Figure 2, except with dots on the bottom. Note that, as part of the resolution of this particular abortion of FR_i , we find inside terms corresponding to all previous abortions.

Proof. When we abort FR_i at the very first step (the bottom-most 6-valent vertex) we get the bottom entry of the table. Now we use induction on which step we abort at. As can be seen in the example above, when one aborts and then resolves the dot, one will get two terms, one of which factors through a lower abortion, and the other of which will provide an interesting new term. This is true also if we abort the first vertex in a

new flip, for we shall have

$$(3.17) \quad \begin{array}{c} \text{Diagram 1} \end{array} = \begin{array}{c} \text{Diagram 2} \end{array} + \begin{array}{c} \text{Diagram 3} \end{array}$$

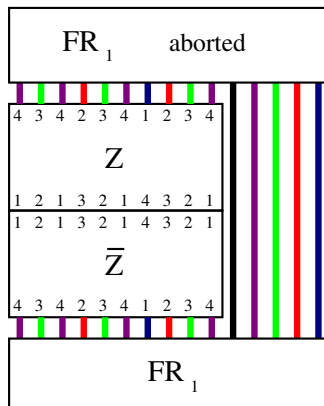
where the first term is a lower abortion. At each stage, therefore, we will ignore lower abortions by induction. In doing so, we only look at one term in each resolution of (2.25), and therefore we may replace our original aborted morphism with what happens when you resolve all dots that touch 6-valent vertices and are eventually left with only dots on the bottom and top.

For the example $n = 5$, the path FR_i has length 10, so there are 10 possible abortions, which we order by the edge aborted from bottom to top. Resolving these modulo lower abortions, we have 10 different diagrams. These factor precisely through the 10 diagrams in Figure 2, in the following order: the rightmost column from bottom to top, then the next rightmost column from bottom to top, and so on. This is a simple thing to check, and we leave it to the reader. There are only two types of resolutions, those in the example above, and those where a dot comes into a flip from above, as in (3.17). \square

Finally, we get a useful result, which explains what happens when we abort the path V_J .

Proposition 3.40. *Let Q_x be the following morphism with bottom boundary s_J : one follows the path V_J , but at some vertex x along the way, instead of following an adjacent edge $x \downarrow y$, one does an aborted 6-valent vertex instead. Then $Q_x \overline{z_J} = 0$.*

Proof. We prove this statement by induction on the number of colors. The base case, where J has two colors, follows from (2.33). So consider the example when $n = 5$, $I = \{1, 2, 3, 4, 5\}$ and $K = \{1, 2, 3, 4\}$. If the vertex x is chosen so that it is part of $\overline{z_K}$, then the morphism factors through $Q_x \overline{z_K}$ where Q_x can be viewed as an aborted path of V_K . Therefore the product is zero by induction. So we may assume that the vertex x is in the sequence of flips at the end of V_J . Therefore, our map looks like



Corollary 3.41. *Suppose that x and y are adjacent vertices along the path V_J , so that $s_J \searrow x \downarrow y \searrow t_J = V_J$. Then the two paths $\varphi = t_J \nearrow s_J \searrow x$ and $\varphi' = t_J \nearrow s_J \searrow y \uparrow x$ have the same path morphism. An equivalent statement holds when one switches s_J and t_J , and reverses all the arrows.*

Corollary 3.42. *Let x be any vertex along the path V_J . Then the path morphisms for $t_J \nearrow s_J \searrow x \nearrow s_J$ and $t_J \nearrow s_J$ are equal. Similarly, the path morphisms for $s_J \searrow t_J \nearrow x \searrow t_J$ and $s_J \searrow t_J$ are equal.*

Corollary 3.43. *Let x be any vertex along the path V_J . Then the path morphisms for $s_J \searrow t_J \nearrow s_J \searrow x$ and $s_J \searrow t_J \nearrow x$ are equal.*

Remark 3.44. We expect a similar statement to Proposition 3.40 and its three corollaries to be true for any vertex in Γ , not just for those on V_J . It should also be relatively easy to prove given the machinery already in place, but would involve more knowledge of what paths are possible in Γ . We choose not to do this explicitly in this paper.

Theorem 3. For $x, y \in \Gamma_{w_J}$, let $\varphi_{x,y}$ be the path morphism $B_x \rightarrow B_y$ corresponding to the path $x \searrow t_J \nearrow s_J \searrow y$. In particular, $\overline{z_J} = \varphi_{t_J, s_J}$. Let $\psi_{x,y}$ be the similar path which goes $x \nearrow s_J \searrow t_J \nearrow y$. In particular, $z_J = \psi_{s_J, t_J}$. Then

$$(3.18) \quad z_J \overline{z_J} z_J = z_J$$

$$(3.19) \quad \varphi_{x,y} = \psi_{x,y}$$

$$(3.20) \quad \varphi_{y,z} \varphi_{x,y} = \varphi_{x,z}$$

See below for a caveat dealing with (3.19).

Proof. Equipped as we are with Corollary 3.41, this theorem is now easy. First we show that $z_J \overline{z_J} z_J = z_J$, or in other words that $s_J \searrow t_J \nearrow s_J \searrow t_J = s_J \searrow t_J$ as path morphisms. But this is just the case $x = t_J$ of Corollary 3.42.

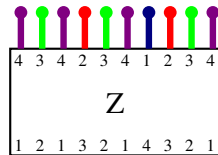
New we show (3.19). Caveat: this proof only works for x, y along the path V_J , but it generalizes to any vertex for which the corollaries above work. We have $\varphi_{x,y} = x \searrow t_J \nearrow s_J \searrow y = x \searrow t_J \nearrow s_J \searrow t_J \nearrow s_J \searrow y$, using the first equality. This path ends with $s_J \searrow t_J \nearrow s_J \searrow y$ which is the same as $s_J \searrow t_J \nearrow y$ by Corollary 3.43. It begins with $x \searrow t_J \nearrow s_J \searrow t_J$ which is the same as $x \nearrow s_J \searrow t_J$ by the same corollary. Thus the morphism is the same as $x \nearrow s_J \searrow t_J \nearrow y = \psi_{x,y}$.

Finally, we show that the maps $\varphi_{x,y}$ form a consistent family of projectors: $\varphi_{y,z} \varphi_{x,y} = x \searrow t_J \nearrow s_J \searrow y \searrow t_J \nearrow s_J \searrow z = x \searrow t_J \nearrow s_J \searrow t_J \nearrow s_J \searrow z = x \searrow t_J \nearrow s_J \searrow z = \varphi_{x,z}$. \square

We have now shown that $\varphi_{x,y}$ is a consistent family of projectors, and thus it picks out some mutual summand of every reduced expression for w_J . We now wish to show that this summand is precisely B_J (we have not even shown yet that the summand is nonzero). Let us temporarily denote the new object in \mathcal{B} corresponding to this family of projectors by the name C .

Proposition 3.45. The R -bimodule $\text{HOM}_{\mathcal{B}}(C, B_{\emptyset})$ is a free left (or right) R -module of rank 1, generated by the map ξ_J of degree d_J which consists of including C into B_x for some reduced expression x of w_J , and then placing dots on each line in B_x . This map is independent of the choice of x .

Example 3.46. (Example: $n = 4$) The map ξ_I :



Proof. First, we observe that the map ξ_J is nonzero, for the specific case of $x = t_J$. Let ξ_{t_J} be the map from $B_{t_J} \rightarrow R$ given by placing d_J dots, one on each line. By definition, ξ_J will be nonzero if and only if $\xi_{t_J} z_J$ is nonzero. The easiest way to prove this is to use the functor from diagrammatics to R -bimodules defined in [3]. It is easy to see that the map z_J preserves 1-tensors, i.e. it sends $1 \otimes 1 \otimes \dots \otimes 1$ to $1 \otimes 1 \otimes \dots \otimes 1$, since the same is true of the 6-valent and 4-valent vertices. The collection of dots sends $1 \otimes 1 \otimes \dots \otimes 1$ to 1. Therefore the map $\xi_{t_J} z_J$ is nonzero, sending the 1-tensor to 1. We know that all Hom spaces in \mathcal{B} are free as left (or right) R -modules, so it is enough to show that every morphism from B_{t_J} to B_\emptyset , when precomposed with z_J , reduces to $\xi_{t_J} z_J$ with some polynomial. If we do this, we will show that the space of morphisms is rank 1, and therefore is determined by the image of $1 \otimes 1 \otimes \dots \otimes 1 \in B_{s_J}$. For another $x \in \Gamma$, the corresponding morphism (if we had defined ξ_J using x) would be $\xi_x \varphi_{s_J, x}$ where ξ_x is the collection of dots. But $\varphi_{s_J, x}$ also preserves 1-tensors, so the overall map sends the 1-tensor to 1. Thus, the map is independent of the choice of x , pending the proof that morphisms are rank 1.

(Example: $n = 4$) We do this using the one-color reduction results of [3]. First, consider the color 1, which is an extremal color. Since it appears only once on the boundary, it reduces to a boundary dot in any morphism. Now consider the color 2, which is an extremal color in the remainder of the morphism (ignoring the 1-colored boundary dot). There are exactly 2 instances of that color on the boundary, so either they are connected by a line, or they both end in boundary dots. However, if they are connected in a line then the morphism must factor through one of the pictures which vanishes due to Proposition (3.33) (only the last column is needed). So both instances of 2 end in boundary dots. Now consider the color 3, which is an extremal color in the remainder of the morphism, so it must form a disjoint union of simple trees. There are 3 instances on the boundary; call them instance 1, 2, 3. If instance m is connected to instance $m + 1$ in the tree, then the morphism factors through a vanishing picture in Proposition (3.33). If this is not the case, but instance m is connected to instance $m + 2$ (in this case, the only possibility is instance 1 connected to instance 3) then instance 2 ends in a dot. However, we know that

$$2 \begin{array}{c} \diagup \\ | \\ \diagdown \end{array} = \begin{array}{c} \diagup \\ | \\ \diagdown \end{array} + \begin{array}{c} \diagup \\ | \\ \diagdown \end{array}$$

thanks to (2.17). Therefore, such a morphism factors through one where m and $m + 1$ are connected, for some m , and vanishes by the above arguments. Thus none of the instances are connected, and they must all end in boundary dots. (If one does not believe that morphisms must be free \mathbb{Z} -modules and is worried about 2-torsion, one can calculate that this morphism is zero more directly, without using the (2.17) trick.) Similarly, considering the color 4, no two instances of 4 on the boundary may be connected, since such a morphism will factor through a morphism where two instances

m and $m+1$ are connected, and this morphism will vanish thanks to Proposition (3.33). Therefore, any nonzero morphism must reduce to φ_J . \square

Of course, one could show that the map was independent of x simply by showing diagrammatically that $\xi_x \varphi_{s_J, x} = \xi_y \varphi_{s_J, y}$ for any $x, y \in \Gamma$. We have bypassed this calculation.

Proposition 3.47. *For any $i \in J$, $C \otimes B_i \cong C\{1\} \oplus C\{-1\}$.*

Proof. Note that

$$\begin{aligned}
 \boxed{J} \quad | &= \begin{array}{|c|} \hline J \\ \hline a_i \\ \hline J \\ \hline \end{array} \quad | = \frac{1}{2} \left(\begin{array}{|c|} \hline J \\ \hline a_i \\ \hline J \\ \hline \end{array} \begin{array}{c} \text{cap} \\ \text{cup} \end{array} + \begin{array}{|c|} \hline J \\ \hline a_i \\ \hline J \\ \hline \end{array} \begin{array}{c} \text{cup} \\ \text{cap} \end{array} \right) \\
 &= \frac{1}{2} \left(\begin{array}{|c|} \hline J \\ \hline a_i \\ \hline J \\ \hline a_i \\ \hline J \\ \hline \end{array} \begin{array}{c} \text{cap} \\ \text{cup} \end{array} + \begin{array}{|c|} \hline J \\ \hline a_i \\ \hline J \\ \hline a_i \\ \hline J \\ \hline \end{array} \begin{array}{c} \text{cup} \\ \text{cap} \end{array} \right)
 \end{aligned}$$

In this calculation, the box labelled J just represents some appropriate projector or idempotent for C . This calculation, proven using Proposition 3.34, decomposes the identity of $C \otimes B_i$ into two orthogonal idempotents, in a similar fashion to (2.18) (checking that they are orthogonal idempotents is also easy with Proposition 3.34). \square

Theorem 4. *The object C is an indecomposable idempotent, whose class in the Grothendieck group is b_J . After applying the functor to R -bimodules, C is isomorphic to B_J .*

Proof. Let c be the class of C in the Grothendieck group. We now know that c lies inside $\mathcal{H}_J \subset \mathcal{H}$, and that $b_i c = (v + v^{-1})c$ for any $i \in J$. This forces c to be inside the ideal of b_J in \mathcal{H}_J , which implies that c is a scalar multiple of b_J . However, thanks to the calculation of Hom spaces in Proposition 3.45 we know that $\varepsilon(c) = v^{d_J}$, and we already knew that $\varepsilon(b_J) = v^{d_J}$. Therefore $c = b_J$. This in turn lets us calculate the graded rank of $\text{END}(C)$, which has a 1-dimensional degree 0 part, and is otherwise concentrated in positive degree. Therefore C is indecomposable. Since indecomposable Soergel bimodules are determined by their image in the Grothendieck group (one can show this using characters; see for instance [14]), we have $C \cong B_J$. \square

Remark 3.48. Let us briefly deal with the case of J a *disconnected* sub-Dynkin diagram, so that $W_J = S_{d_1} \times S_{d_2} \times \dots \times S_{d_k}$. The longest element is just the product of the longest element of each S_{d_i} , and similarly, B_J is just the tensor product of $B_{S_{d_i}}$. The graph Γ_{w_J} for this parabolic is just a product of the graphs for the longest element of each S_{d_i} , which has a large number of disjoint squares but is otherwise not particularly

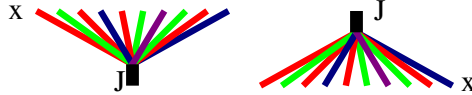
complicated. If we let s_J (the source) be the concatenation of $s_{S_{d_i}}$ (and the same for t), then we may view the path morphism from $s_J \rightarrow t_J$ diagrammatically as the horizontal concatenations of the path morphism for each component. To define a_i for J , define it for the connected subgraph of which i is a part, and then extend it via the identity map to the remainder of J (thanks to distant sliding rules, it has all the same properties). The main results and theorems hold true for disconnected J as well.

3.5. Augmented Graphical Calculus. We may now use Claim 2.11 to give ourselves a graphical calculus for \mathcal{B}_{gBS} by adding inclusion and projection maps accordingly. Recall that \mathcal{B}_{gBS} is the partial idempotent completion of \mathcal{B}_{BS} which adds all B_J for parabolic subsets J . Since B_J for J disconnected is a tensor product of various B_K for K connected, we need only adjoin B_J for J connected. As usual, we abuse notation and write \mathcal{B}_{gBS} for both the category of R -bimodules and the diagrammatic presentation thereof.

Definition 3.49. Let \mathcal{B}_{gBS} be the graded monoidal category presented diagrammatically as follows. Objects are sequences $J_1 J_2 \dots J_d$ of connected subsets of $I = \{1, \dots, n\}$. When $J = \{j\}$ is a single element, we write the element j instead of writing J , and identify it with an object in \mathcal{B}_{BS} . We also denote the object as $B_{J_1 J_2 \dots J_d}$. We draw the identity of B_J as follows:



The generating morphisms are the usual generators of \mathcal{B}_{BS} , in addition to *projections* and *inclusions*. These are maps to/from B_J from/to B_x where x is any reduced expression for w_J , the longest element of W_J .



The relations are those relations of \mathcal{B}_{BS} as well as

$$(3.21) \quad \begin{array}{c} \text{A diamond shape formed by multiple colored lines (red, green, blue, purple) connecting a small black square labeled J at the bottom to a point labeled x at the top.} \end{array} = \begin{array}{c} \text{A single vertical black line with a small black square at its base, labeled J below it.} \end{array} \quad \begin{array}{c} \text{A diagram showing a fan of colored lines (red, green, blue, purple) connecting a point labeled x at the top to a small black square labeled J at the bottom, and another fan of colored lines connecting a point labeled y at the bottom to the same small black square labeled J.} \end{array} = \begin{array}{c} \text{A rectangular box containing the symbol } \varphi_{y,x} \text{ with a point labeled x at the top and a point labeled y at the bottom.} \end{array}$$

Theorem 5. *This diagrammatic category is equivalent to the partial idempotent completion \mathcal{B}_{gBS} in R -bimodules.*

Proof. This is now obvious. □

Let us discuss quickly the functor which realizes this equivalence. On objects it is easily defined: it sends J to B_J . On morphisms, we need only define the image of the

projections and inclusions under the functor, which are degree zero maps, determined up to an invertible scalar. We choose the scalars so that the projection map sends $1 \otimes 1 \otimes \dots \otimes 1 \in B_x$ to $1 \otimes 1 \in B_J$ for any $x \in \Gamma$, and so that the inclusion map sends $1 \otimes 1 \in B_J$ to $1 \otimes 1 \otimes \dots \otimes 1 \in B_x$. Since the transition maps $\varphi_{x,y}$ send 1-tensors to 1-tensors, this system of scalars is consistent and the functor is well-defined. Note that the image of B_J in B_x is precisely those tensors spanned by $f \otimes 1 \otimes 1 \otimes \dots \otimes 1 \otimes g$, which we call *extremal tensors*. In other words, the image is generated as a bimodule by the 1-tensor. Since any transition map $\varphi_{x,y}$ factors through B_J , it must send arbitrary tensors to extremal tensors. To determine what the projection map will do to an arbitrary tensor $f_1 \otimes f_2 \otimes \dots \otimes f_{d_J+1}$, we may apply any transition map $\varphi_{x,y}$ (which is explicit, albeit annoying to compute) to obtain an extremal tensor, and then map the extremal tensor to B_J by the rule $f \otimes 1 \otimes \dots \otimes 1 \otimes g \mapsto f \otimes g$.

As intimated previously, it will be more useful and intuitive to introduce new pictures to represent maps which can already be obtained from the generators above, and in doing so we “augment” our diagrammatics. Any relations between these further pictures need only be checked in \mathcal{B}_{BS} using the relations already mentioned. The remainder of this chapter will introduce further pictures and explore some of their basic properties. We will place each new picture in a definition, along with its defining relation, and follow it with discussion, saving the most difficult discussion for the end. We will then collect all the new generators and relations at the end for the convenience of the reader.

In theory, all the relations stated in this section can be checked explicitly using the diagrammatic relations of \mathcal{B}_{BS} , mostly using the calculations of the previous sections. Some of these checks are huge pains in the neck though. Thankfully, we have Theorem 5 which means that we already know the graded dimension of Hom spaces between objects in \mathcal{B}_{gBS} , and we have a functor to R -bimodules. Thus, if we have two different pictures which represent a map of a certain degree, and the dimension of the Hom space in that degree is 1, then they are equal up to a scalar, and the scalar may often be quickly checked by looking at what the map does to a 1-tensor. This saves me a lot of work and you a lot of reading: we know a priori that certain relations can be derived from the diagrammatic calculus, but no one wants to see it done explicitly unless the calculation is pretty.

When calculating these graded dimensions, just remember that $\varepsilon(b_J) = v^{d_J}$, $b_J^2 = [J] b_J$, and $b_J b_i = [2] b_J$ when $i \in J$. For instance, $\text{END}(B_J)$ has graded dimension $v^{d_J} [J]$, so it has a 1-dimensional space of degree 0 morphisms, generated by the identity map.

Definition 3.50. The *thick cup* and *thick cap* express the biadjointness of J with itself.

$$(3.22) \quad \text{cup} = \text{thick cup} \quad \text{cap} = \text{thick cap}$$

Thanks to the self-biadjointness of B_i , we know that $B_{\underline{i}}$ is biadjoint to $B_{\omega(\underline{i})}$. For an arbitrary element $v \in S_n$ we do not know explicitly what B_v is, but we do know that it often fails to be self-dual. For instance, when $v = s_i s_j$ for i, j adjacent, $B_v \cong B_i \otimes B_j$, and therefore B_v is biadjoint to $B_{v^{-1}}$ and not itself. However, for the longest element w_J of a parabolic subgroup, the fact that $\omega(b_J) = b_J$ lifts to the fact that B_J is actually self-dual. This should not be terribly surprising: for any reduced expression \underline{i} of w_J , $\omega(\underline{i})$ is also a reduced expression for w_J . This enables us to define the thick cups and caps easily as above. It is trivial to show the biadjointness relation (using the fact that $\varphi_{x,y}$ upside-down is $\varphi_{y,x}$).

$$(3.23) \quad \text{thick cup} = \text{thick dot} = \text{thick cap}$$

Definition 3.51. The *thick dot* is obtained by choosing a reduced expression x for w_J and composing $B_J \rightarrow B_x \rightarrow B_\emptyset$, where the latter map consists of a dot on every strand.

$$(3.24) \quad \text{thick dot} = \text{multi-colored fan}$$

This was the map called ξ_J in Proposition 3.45. From that proposition we have

Claim 3.52. *The map above is nonzero, and independent of the choice of x , so it is well defined. It is the generator of $\text{Hom}_{\mathcal{B}}(B_J, B_\emptyset)$.*

The definition of an upside-down thick dot is the same, only flipped upside-down. The cyclicity of thick dots is quite clear.

$$(3.25) \quad \text{thick cup with dot} = \text{thick dot} = \text{thick cap with dot}$$

Definition 3.53. The *thick crossing* exists only when J and K are *distant*, that is, every index inside them is distant. It agrees with the usual 4-valent crossing when $J = \{j\}$ and $K = \{k\}$.

$$(3.26) \quad \text{thick crossing} = \text{multi-colored crossing}$$

This crossing gives the isomorphism $B_J \otimes B_K \cong B_K \otimes B_J$ for J, K distant. There will be distant sliding rules, which we will present in full after all the new pictures have been presented. Once again, it is obvious that the thick crossing is cyclic.

$$(3.27) \quad \begin{array}{c} \text{Pink loop with a crossing labeled } J \text{ and } K \end{array} = \begin{array}{c} \text{Crossing of black and pink lines} \end{array} = \begin{array}{c} \text{Black loop with a crossing labeled } J \end{array}$$

Definition 3.54. The *thick trivalent vertex* exists only when $i \in J$. It agrees with the usual trivalent vertex when J is a singleton. Thick trivalent vertices may be *right-facing* as in the picture below, or may be *left-facing* (sending the extra index i off to the left).

$$(3.28) \quad \begin{array}{c} \text{Thick vertical line with a teal line crossing it} \end{array} = \begin{array}{c} \text{Box labeled } a_i \text{ with multiple colored lines entering and exiting} \end{array}$$

The utility of these maps has already been seen in the proofs of the previous section. These relations rephrase Proposition 3.34.

$$(3.29) \quad \begin{array}{c} \text{Thick vertical line with a teal line crossing it} \end{array} = \begin{array}{c} \text{Thick vertical line} \end{array}$$

$$(3.30) \quad \begin{array}{c} \text{Thick vertical line with a teal line crossing it} \end{array} = \begin{array}{c} \text{Thick vertical line with a teal line crossing it} \end{array}$$

$$(3.31) \quad \begin{array}{c} \text{Thick vertical line with a teal line crossing it} \end{array} = \begin{array}{c} \text{Thick vertical line with a teal line crossing it} \end{array}$$

$$(3.32) \quad \begin{array}{c} \text{Thick vertical line with a teal line crossing it} \end{array} = \begin{array}{c} \text{Thick vertical line with a teal line crossing it} \end{array}$$

$$(3.33) \quad \begin{array}{c} \text{Thick vertical line with a teal line crossing it} \end{array} = \begin{array}{c} \text{Thick vertical line with a teal line crossing it} \end{array}$$

In addition, a quick comparison of a_i when expressed on the right for s_J^R and on the left for t_J^L will convince the reader of the cyclicity of the thick trivalent vertex.

$$(3.34) \quad \begin{array}{c} \text{U} \\ \text{U} \end{array} = \begin{array}{c} \text{U} \\ \text{U} \end{array}$$

Rephrasing the isomorphism $B_J \otimes B_i \cong [2] B_J$ in terms of thick trivalent vertices is easy given from Proposition 3.47. We leave it to the reader to prove that the thick trivalent vertex, viewed as a morphism $B_J \otimes B_i \rightarrow B_J$, is the unique morphism of degree -1 up to scalar, and it sends $f \otimes g \otimes h \mapsto f \otimes \partial_i(g)h$ (Hint: use a reduced expression for w_J ending in i).

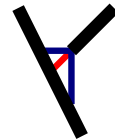
Now, we wish to give a diagrammatic relation corresponding to the isomorphism $B_J \otimes B_J \cong [J] B_J$, and so we will need a number of projection and inclusions maps from/to $B_J \otimes B_J$ to/from B_J of various different degrees. We construct these in a fashion entirely akin to the isomorphism $B_i \otimes B_i \cong [2] B_i$. First, we find the projection/inclusion of minimal degree, and draw it as a trivalent vertex.

Definition 3.55. The *very thick trivalent vertex* is constructed by choosing a reduced expression x for w_J , and using the corresponding sequence of thick trivalent vertices. It has degree $-d_J$.

$$(3.35) \quad \begin{array}{c} \text{---} \\ \text{---} \end{array} = \begin{array}{c} \text{---} \\ \text{---} \end{array}$$

Once again, the reader should be easily convinced that this map does not depend on the choice of x . After all, 6-valent and 4-valent vertices may be pushed in and out of the sequence of thick trivalent vertices, as in (3.31) and (3.32). Even had we not appended the projection to B_J on the right of the diagram, but had instead B_x on the right boundary, the map still would have factored through the B_J summand of B_x , because one could “pull” any transition map out of the thick line using (3.31) and (3.32) repeatedly.


Moreover, it is true, but not immediately obvious, that the morphism is cyclic, or equivalently that it didn’t matter which of the three strands was chosen to be special. One could show this diagrammatically, or more easily by using the functor to bimodules. Recall that there is a unique morphism of degree $-d_J$ from $B_J \rightarrow B_J \otimes B_J$ up to scalar,

and similarly from $B_J \otimes B_J \rightarrow B_J$. Consider the map . It is easy to observe

that this map sends the 1-tensor to the 1-tensor, and so does its horizontal flip, so the map is equal to its horizontal flip.

Definition 3.56. Let \underline{i} be a reduced expression of w_J . Then $\partial_{\underline{i}} \stackrel{\text{def}}{=} \partial_{i_1} \dots \partial_{i_{d_J}}$, the composition of Demazure operators, is independent of the choice of reduced expression.

The result is a degree $-2d_J$ map from $R \rightarrow R^J$ which is R^J -linear, denoted ∂_J and also called a *Demazure operator*.

Consider . This map sends $f \otimes g \otimes h \mapsto f \otimes \partial_J(g)h$, and so does its horizontal

flip, so the two maps are equal. Together with the equality above, we have shown the cyclicity of the very thick trivalent vertex.

$$(3.36) \quad \text{U-shape} = \text{Y-shape} = \text{inverted U-shape}$$

Before we go any further, we digress to display the *thick distant sliding property*. Everything other than J is assumed to be distant from J . The corresponding calculations in \mathcal{B}_{BS} are all trivial, coming from the usual distant sliding property.

$$(3.37) \quad \begin{array}{ccc} \text{K} \text{ (curved)} \text{ J} & = & \text{K} \text{ (vertical)} \text{ J} \text{ (vertical)} \\ \text{J} \text{ (horizontal)} \text{ K} \text{ (curved)} & = & \text{J} \text{ (horizontal)} \text{ K} \text{ (vertical)} \\ \text{K} \text{ (curved)} \text{ L} & = & \text{K} \text{ (vertical)} \text{ L} \text{ (vertical)} \\ \text{J} \text{ (horizontal)} \text{ K} \text{ (curved)} & = & \text{J} \text{ (horizontal)} \text{ K} \text{ (vertical)} \\ \text{K} \text{ (curved)} \text{ L} & = & \text{K} \text{ (vertical)} \text{ L} \text{ (vertical)} \\ \text{J} \text{ (horizontal)} \text{ K} \text{ (curved)} & = & \text{J} \text{ (horizontal)} \text{ K} \text{ (vertical)} \end{array}$$

Now we investigate the very thick trivalent vertex and the thick trivalent dot more thoroughly. The first statement is that they give B_J the structure of a Frobenius algebra object in \mathcal{B}_{BS} . In addition to the cyclicity properties already mentioned, this requires only two more relations.

$$(3.38) \quad \text{Y-shape with dot} = \text{vertical line} = \text{inverted Y-shape with dot}$$

$$(3.39) \quad \text{Y-shape} = \text{X-shape}$$

These are easy to check. For both relations, the equalities must be true up to scalar by a calculation of the graded dimension of Hom spaces, and the scalar is 1 because both sides send a 1-tensor to a 1-tensor (this is true of the appropriate twist of (3.39)). Here is another easy relation, also in some sense a “unit” relation:

$$(3.40) \quad \begin{array}{c} \text{blue line} \\ \text{thick dot} \\ \text{blue line} \end{array} = \begin{array}{c} \text{blue line} \\ \text{thick dot} \\ \text{blue line} \end{array}$$

Before we go on, it will be useful to make a brief aside about Frobenius algebras and Demazure operators. We can see that B_J is a Frobenius algebra object in \mathcal{B}_{gBS} , but this is because R is a (symmetric) Frobenius algebra over R^J . In particular, the Demazure operator ∂_J is the nondegenerate trace, so that there is some set of polynomials $\{g_r\}$ which is a basis for R as an R^J -module (free of graded rank $[J]$), and some other basis $\{g_r^*\}$ as well, for which $\partial_J(g_r g_q^*) = \delta_{r,q}$. These polynomials are indexed by $r \in W_J$, and g_r has degree $2l(r)$, while g_r^* has degree $2(d_J - l(r))$. We may as well assume that $g_1 = g_{w_J}^* = 1$.

Claim 3.57. *The element $\beta = \sum_{w_J} g_r \otimes g_r^* \in B_J$ satisfies $f\beta = \beta f$ for any $f \in R$.*

This is a standard fact about Frobenius algebras. One obtains the same element β regardless of which basis and dual basis we choose. Alternatively, we may define β as the image of $1 \in R$ under the thick dot.

Remark 3.58. In type A, there is a nice choice of basis and dual basis known as *Schubert polynomials*. The advantage of Schubert polynomials in type A is that one may choose other Schubert polynomials to form the dual basis. However, we never make any assumptions about the choice of basis in this paper.

The internet contains numerous easily-obtained resources on Frobenius algebras and Schubert polynomials.

Remember that the very thick trivalent vertex, seen as a map from $R \otimes_{R^J} R \otimes_{R^J} R \{-2d_J\} = B_J \otimes B_J \rightarrow B_J$, applies the Demazure operator ∂_J to the middle term, while seen as a map from $B_J \rightarrow B_J \otimes B_J$, it adds 1 as the middle term. We now list some relations which can be deduced from the previous discussion without too much effort, and are obvious generalizations of the one-color relations for \mathcal{B}_{BS} . Recall that a box with $f \in R$ inside represents multiplication by f .

$$(3.41) \quad \begin{array}{c} \text{thick line} \\ \text{circle} \\ \text{thick line} \end{array} \begin{array}{c} \boxed{f} \end{array} = \begin{array}{c} \text{thick line} \\ \text{thick line} \end{array} \begin{array}{c} \boxed{\partial_J(f)} \end{array}$$

$$(3.42) \quad \begin{array}{c} \text{thick line} \\ \text{thick dot} \\ \text{thick line} \end{array} = \sum \begin{array}{c} \boxed{g_r} \end{array} \begin{array}{c} \text{thick line} \\ \text{thick line} \end{array} \begin{array}{c} \boxed{g_r^*} \end{array}$$

$$(3.43) \quad \begin{array}{|c|} \hline \\ \hline \end{array} \begin{array}{|c|} \hline \\ \hline \end{array} = \sum \begin{array}{c} \begin{array}{|c|} \hline \\ \hline \end{array} \begin{array}{|c|} \hline \\ \hline \end{array} \\ \begin{array}{|c|} \hline \\ \hline \end{array} \end{array} \begin{array}{c} \boxed{g_r} \\ \boxed{g_r^*} \end{array}$$

The last relation expresses the decomposition $B_J \otimes B_J \cong [J] B_J$.
We make one further extension of the calculus.

Definition 3.59. The *generalized thick trivalent vertex*, with top and bottom boundary B_J and right boundary B_K for $K \subset J$, is constructed in the same fashion as the very thick trivalent vertex, and generalizes both the very thick trivalent vertex and the thick trivalent vertex.

$$(3.44) \quad \begin{array}{|c|} \hline J \\ \hline \\ \hline J \\ \hline \end{array} \begin{array}{|c|} \hline \\ \hline \end{array} K = \begin{array}{|c|} \hline J \\ \hline \\ \hline \\ \hline \end{array} \begin{array}{c} \text{thick line} \\ \text{thick line} \end{array} K$$

The reader should easily be able to generalize the previous discussion to this new picture. In particular, it is cyclic, satisfies various associativity properties akin to (3.30) and (3.33), a unit axiom akin to (3.38) or (3.29), and another one akin to (3.40). It has distant sliding rules, applies the Demazure operator ∂_K to the middle term in $B_J \otimes B_K$, and can be used to express the isomorphism $B_J \otimes B_K \cong [K] B_J$.

Remark 3.60. In fact, the category \mathcal{B}_{gBS} is generated entirely by generalized thick trivalent vertices, thick dots, and thick crossings. It is not too hard to see that the other maps in \mathcal{B}_{gBS} , namely the 6-valent vertex and the projections and inclusions, can actually be constructed out of these. Below, the thick line represents $J = \{1, 2\}$.

$$\begin{array}{c} \text{thick line} \\ \text{thick line} \end{array} = \begin{array}{c} \text{thick line} \\ \text{thick line} \end{array} \quad \begin{array}{c} \text{thick line} \\ \text{thick line} \end{array} = \begin{array}{c} \text{thick line} \\ \text{thick line} \end{array}$$

There are presumably many more interesting relations to be found, but these shall be good enough for now. Finding the relations which intertwine thick lines in interesting ways is a more difficult problem.

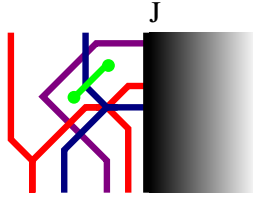
4. INDUCED TRIVIAL REPRESENTATIONS

Recall from Sections 2.1 and 2.2 that the full subcategory of $R - R^J$ -bimodules $\text{Hom}_{\text{BS}}(R^J, R)$ (or rather, its idempotent completion) is a categorification of the induced (left) representation T_J , which is the left ideal generated by b_J in \mathcal{H} . To categorify this, we wish to use the “left ideal” generated by B_J in \mathcal{B}_{gBS} or $\mathcal{B}_{\text{BS}}(B_J)$. That is, we consider all pictures which have a thick line labelled J appearing on the right. We may think of the remainder of the diagram as a picture in \mathcal{B}_{BS} , and view the thick line on the right

as some sort of “membrane” which interacts in a specific way with the morphisms in \mathcal{B}_{BS} .

Definition 4.1. Let \mathcal{T}_J be the category defined as follows. Objects are sequences \underline{i} of indices in I , just as for \mathcal{B}_{BS} . Morphisms between \underline{i} and \underline{j} are given by (linear combinations of) pictures on the plane, with appropriate top and bottom boundary, which include a membrane on the right labelled J . These pictures are constructed out of the generators of \mathcal{B}_{BS} and the *left-facing* thick trivalent vertex, which is the only interaction with the membrane. The relations between these morphisms are given by those relations of \mathcal{B}_{BS} as well as the left versions of (3.29), (3.30), (3.31), and (3.32). This category is equipped with an obvious monoidal action of \mathcal{B}_{BS} on the left. We view morphisms as being equipped with the structure of a left R -module, by placing double dots on the left of the diagram, and a right R^J -module, by placing symmetric polynomials immediately to the left of the membrane.

Here is an example morphism, for some J containing $\{1, 2, 4\}$.



Remark 4.2. The right action of R^J on morphisms is well-defined. That is, it does not matter in which region to the left of the membrane one places the polynomial, since the polynomial is symmetric in W^J and therefore slides freely across any line labelled $i \in J$. Only these lines may be involved in thick trivalent vertices with the membrane, so only these lines separate the regions in question.

Definition 4.3. There is a functor from \mathcal{T}_J to $\text{Hom}_{\text{BS}}(R^J, R)$ defined as follows. The object \underline{i} is sent to $B_{\underline{i}}$, restricted so that it is a right R^J -module instead of a right R -module. Morphisms using usual Soergel diagrammatics are sent to their usual counterparts in \mathcal{B}_{BS} , which are obviously also right R^J -module maps. The image of the thick trivalent vertex is:

$$(4.1) \quad \begin{array}{ccc} \text{Diagram} & R \otimes_{R^i} R & f \otimes 1 \\ \uparrow & \uparrow & \uparrow \\ & R & f \end{array}$$

$$(4.2) \quad \begin{array}{ccc} \text{Diagram} & R & f \partial_i(g) \\ \uparrow & \uparrow & \uparrow \\ & R \otimes_{R^i} R & f \otimes g \end{array}$$

These are clearly maps of left R -modules and right R^J -modules.

Definition 4.4. There is a functor from \mathcal{T}_J to the diagrammatic version of \mathcal{B}_{gBS} defined as follows. The object \underline{i} in \mathcal{T}_J is sent to $\underline{i}J$ in \mathcal{B}_{gBS} . The map is given on morphisms by interpreting the membrane as a thick line labelled J , with nothing to the right of it.

Claim 4.5. *These functors are well defined, and preserve the $R - R^J$ -bimodule structure of Hom spaces. The composition of functors from \mathcal{T}_J to the diagrammatic \mathcal{B}_{gBS} and then to the R -bimodule version is equal to the composition of functors from \mathcal{T}_J to $\text{Hom}_{\text{BS}}(R^J, R)$ and then to \mathcal{B}_{gBS} by inducing from R^J to R .*

Proof. Given the calculations and remarks of the previous chapter, this is entirely obvious. \square

Remark 4.6. Consider the map $\text{Hom}_{\mathcal{T}_J}(B_{\underline{i}}, B_{\underline{j}}) \rightarrow \text{Hom}_{\mathcal{B}_{\text{gBS}}}(\underline{i}J, \underline{j}J)$ given by this functor. We will show that this map is an injection. It is not a surjection, however, essentially because it misses polynomials to the right of the thick line. For instance, consider the left side of (3.42). This does not correspond to a map in \mathcal{T}_J from $\emptyset \rightarrow \emptyset$ because it factors in \mathcal{B}_{gBS} through an object \emptyset without B_J on the right, so can not be described with a membrane. Thanks to (3.42), however, we may express it as a linear combination of morphisms in the image of \mathcal{T}_J but with added polynomials on the right. There are other morphisms from B_J to B_J which we must also exclude: including into B_x , breaking some of the lines, and projecting back to B_J would give such a morphism. From the Soergel bimodule description, we know that $\text{Hom}_{\mathcal{B}}(B_J, B_J)$ consists of double dots on either side of a thick line, and all these excluded morphisms will come from the extra terms created while forcing double dots from the left to the right of the thick line. As we shall see, $\text{Hom}_{\mathcal{T}_J}(\emptyset, \emptyset)$ will consist only of double dots on the left side of the membrane.

Recall from Section 2.2 that for two $R - R^J$ -bimodules X, Y in $\text{Hom}_{\text{BS}}(R^J, R)$ we have an R -bimodule isomorphism $\text{Hom}_{\mathcal{B}}(X \otimes_{R^J} R, Y \otimes_{R^J} R) \cong \text{Hom}_{\text{Hom}_{\text{BS}}(R^J, R)}(X, Y) \otimes_{R^J} R$.

Theorem 6. *The functor from \mathcal{T}_J to $\text{Hom}_{\text{BS}}(R^J, R)$ is an equivalence of categories.*

Proposition 4.7. *There is an R -bimodule isomorphism of Hom spaces $\text{Hom}_{\mathcal{B}_{\text{gBS}}}(\underline{i}J, \underline{j}J) \cong \text{Hom}_{\mathcal{T}_J}(\underline{i}, \underline{j}) \otimes_{R^J} R$*

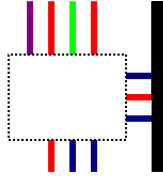
Corollary 4.8. *The space $\text{Hom}_{\mathcal{T}_J}(\underline{i}, \underline{j})$ is a free left R -module of graded rank $v^{-d_J} \varepsilon(b_J b_{\underline{i}} b_{\omega(\underline{j})})$.*

Proof. For the proposition, the map from the right side to the left is obvious diagrammatically: we send a morphism in \mathcal{T}_J to the corresponding morphism in \mathcal{B}_{gBS} , and we send a polynomial in R to the corresponding double dots to the *right* of the thick line. Any polynomial in R^J may slide freely across the thick line, so the map is well defined on the tensor product. This map commutes with the functors to R -bimodules.

First we show that the Hom space map is surjective. Consider an arbitrary morphism in \mathcal{B}_{gBS} from $\underline{i}J$ to $\underline{j}J$. We can merge the two J inputs (top right, bottom right) using the relation (3.43).

Then, using the definition in \mathcal{B}_{gBS} of the very thick trivalent vertex, we may rewrite the equation as above. The lines emanating from the thick line in the final picture form some reduced expression x of w_J . The morphism inside the box may be different in each term of the sum. Note that the morphism inside the box is a morphism between objects in \mathcal{B}_{BS} , and since \mathcal{B}_{BS} includes fully faithfully into its partial idempotent completion \mathcal{B}_{gBS} , we may assume that the morphism inside the box only uses diagrams from \mathcal{B}_{BS} (i.e. no further thick lines are present). Therefore, the result is in the image of the Hom space map.

In fact, the calculation above implies that $\text{Hom}_{\mathcal{B}_{\text{gBS}}}(\underline{\mathbf{i}}J, \underline{\mathbf{j}}J)$ is precisely $M \otimes_{R^J} R$, where “ $M = \text{Hom}_{\mathcal{B}_{\text{BS}}}(\underline{\mathbf{i}}x, \underline{\mathbf{j}})\varphi_{x,x}$ ” is the space of all morphisms in \mathcal{B}_{BS} which have boundary $\underline{\mathbf{i}}x\omega(\underline{\mathbf{j}})$ reading around the circle (i.e. morphisms fitting inside the box) and which are unchanged when composed with the transition map $\varphi_{x,x}$ along the x input. Any morphism in \mathcal{T}_J is equal to one of the following form, because regardless of what thick trivalent vertices exist at the start, one may stretch additional lines with dots out from the thick line, using (3.29), and then apply various of the thick trivalent properties until the trivalent vertices exiting the thick line are precisely x .



Therefore we have a surjective map $M \rightarrow \text{Hom}_{\mathcal{T}_J}(\underline{\mathbf{i}}, \underline{\mathbf{j}})$, which provides the inverse of the Hom space map above. This proves the proposition.

Because the various functors compose properly as in Claim 4.5, it would be impossible for the above map to be an isomorphism unless the functor from $\mathcal{T}_J \rightarrow \text{Hom}_{\text{BS}}(R^J, R)$ is fully faithful. This proves the theorem. Thus, too, is the Corollary proven, since Hom spaces in \mathfrak{B} are free as right or left modules, and graded ranks in $\text{Hom}_{\text{BS}}(R^J, R)$ are known already to agree with this formula (see Section 2.2). \square

REFERENCES

- [1] D. Bar-Natan and S. Morrison, The Karoubi envelope and Lee's degeneration of Khovanov homology, *Algebr. Geom. Topol.* **6** (2006), 1459–1469. arXiv:math/0606542.
- [2] B. Elias, A Diagrammatic Temperley-Lieb categorification, preprint 2010, arXiv:1003.3416.
- [3] B. Elias and M. Khovanov, Diagrammatics for Soergel categories, preprint 2009, arXiv:0902.4700.
- [4] B. Elias and D. Krasner, Rouquier complexes are functorial over braid cobordisms, preprint 2009, arXiv:0906.4761.
- [5] M. Khovanov and A. Lauda, A diagrammatic approach to categorification of quantum groups I, *Represent. Theory* **13** (2009), 309–347. arXiv:0803.4121.
- [6] M. Khovanov and A. Lauda, A diagrammatic approach to categorification of quantum groups II, preprint 2008, arXiv:0804.2080. To appear in *Trans. Amer. Math. Soc.*
- [7] M. Khovanov, A. Lauda, M. Mackaay and M. Stošić, Extended graphical calculus for categorified quantum $\mathfrak{sl}(2)$, preprint 2010, arXiv:1006.2866.
- [8] A. Lauda, A categorification of quantum $\mathfrak{sl}(2)$, preprint 2008, arXiv:0803.3652. To appear in *Adv. Math.*
- [9] N. Libedinsky, New bases of some Hecke algebras via Soergel bimodules, preprint 2009, arXiv:0907.0031.
- [10] Y. Manin and V. Schechtman, Arrangements of Hyperplanes, Higher Braid Groups and Higher Bruhat Orders, *Advanced Studies in Pure Math.* **17** (1989), 289–308.
- [11] V. Mazorchuk and C. Stroppel, Categorification of (induced) cell modules and the rough structure of generalised Verma modules, *Adv. Math.* **219** (2008), no. 4, 1363–1426. arXiv:math/0702811.
- [12] W. Soergel, Category \mathcal{O} , perverse sheaves and modules over the coinvariants for the Weyl group, *J. Amer. Math. Soc.* **3** (1990), no. 2, 421–445.
- [13] W. Soergel, The combinatorics of Harish-Chandra bimodules, *J. Reine Angew. Math.* **429** (1992), 49–74.
- [14] W. Soergel, Kazhdan-Lusztig polynomials and indecomposable bimodules over polynomial rings, *J. Inst. Math. Jussieu* **6** (2007), no. 3, 501–525. English translation available on Soergel's webpage.
- [15] M. Varagnolo and E. Vasserot, Canonical bases and Khovanov-Lauda algebras, preprint 2009, arXiv:0901.3992.
- [16] G. Williamson, Singular Soergel Bimodules, PhD Thesis 2008. Can be found on Williamson's webpage.

Ben Elias, Department of Mathematics, Columbia University, New York, NY 10027
 email: belias@math.columbia.edu